The Time Evolution of Pulsar Wind Nebulae

Okkie de Jager, S. Ferreira (NWU, South Africa)

Science with the New Generation of High Energy Gamma-Ray Experiments (6th Workshop), Padova
8 – 10 October 2008

NORTH-WEST UNIVERSITY
YUNIBESITI YA BOKONE-BOPHIRIMA
NOORDWES-UNIVERSITEIT

science & technology
Department:
Science and Technology
REPUBLIC OF SOUTH AFRICA

NRF

H.E.S.S.

Contents

- Galactic Latitude distribution of HESS sources
  - Methanol Maser – leading to core collapse stars
  - Molecular gas (CO)
  - Offset PWN statistics (reverse shocks due to anisotropic ISM density)
  - Conversion efficiencies –Photon index distribution – the cooling effect.
- MHD Simulation Code
  - Evolution of Magnetic field strength of PWN.
- Importing Time dependent Radiation model
- Multiwavelength SED of G21.5-0.9.
- Time evolution of MWL spectrum of G21.5-0.9
- Evolutionary Tracks in X-rays and TeV
- The Calirometric-Relic effect.
- KES 75
- Conclusions

Galactic (b) distribution of HESS Sources: L>200 deg & L<60 deg (Southern Hemisphere)

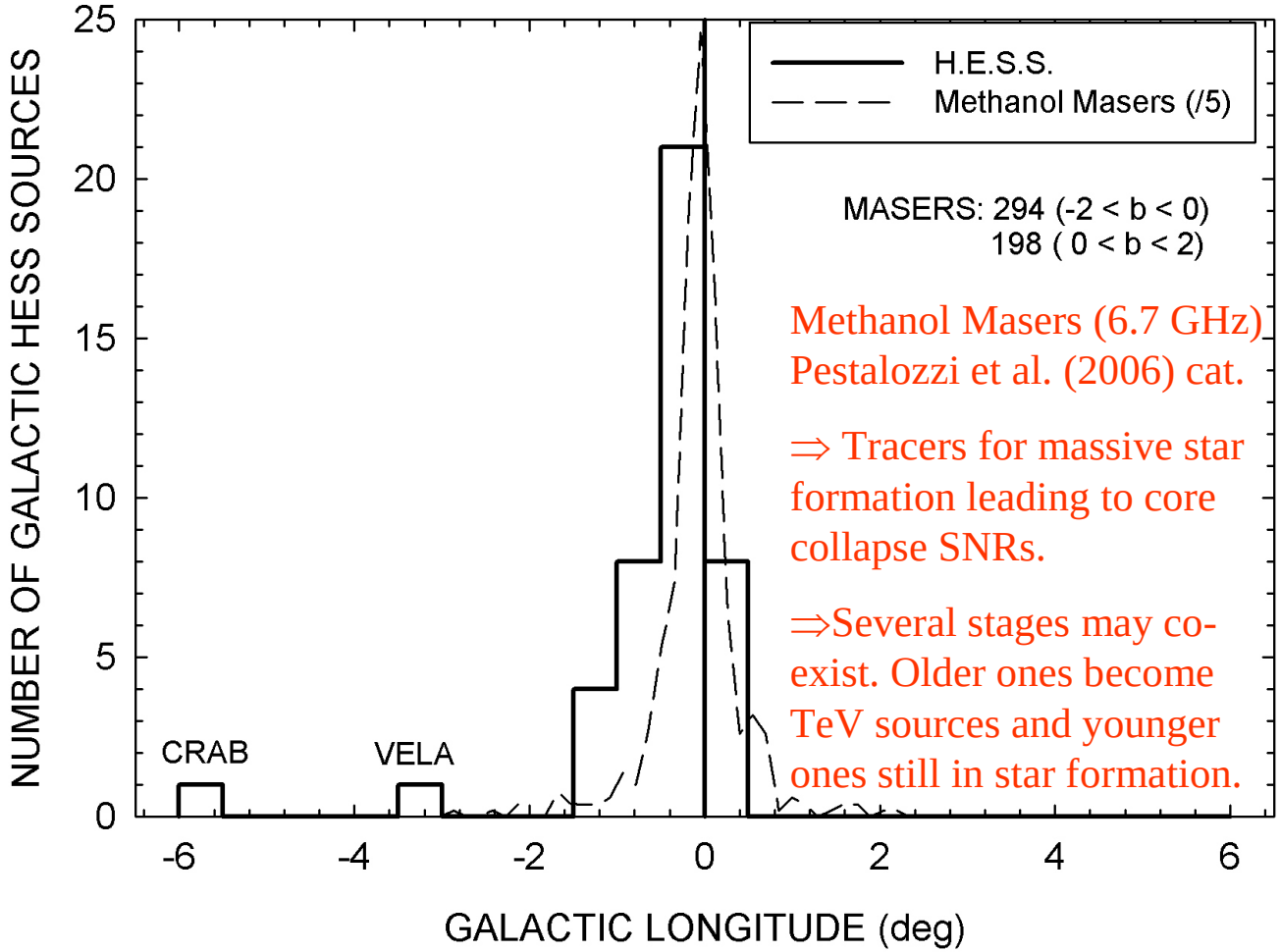

Methanol Masers (6.7 GHz) Pestalozzi et al. (2006) cat.

⇒ Tracers for massive star formation leading to core collapse SNRs.

⇒Several stages may co-exist. Older ones become TeV sources and younger ones still in star formation.

Galactic (b) distribution of HESS Sources: L>200 deg & L<60 deg (Southern Hemisphere)

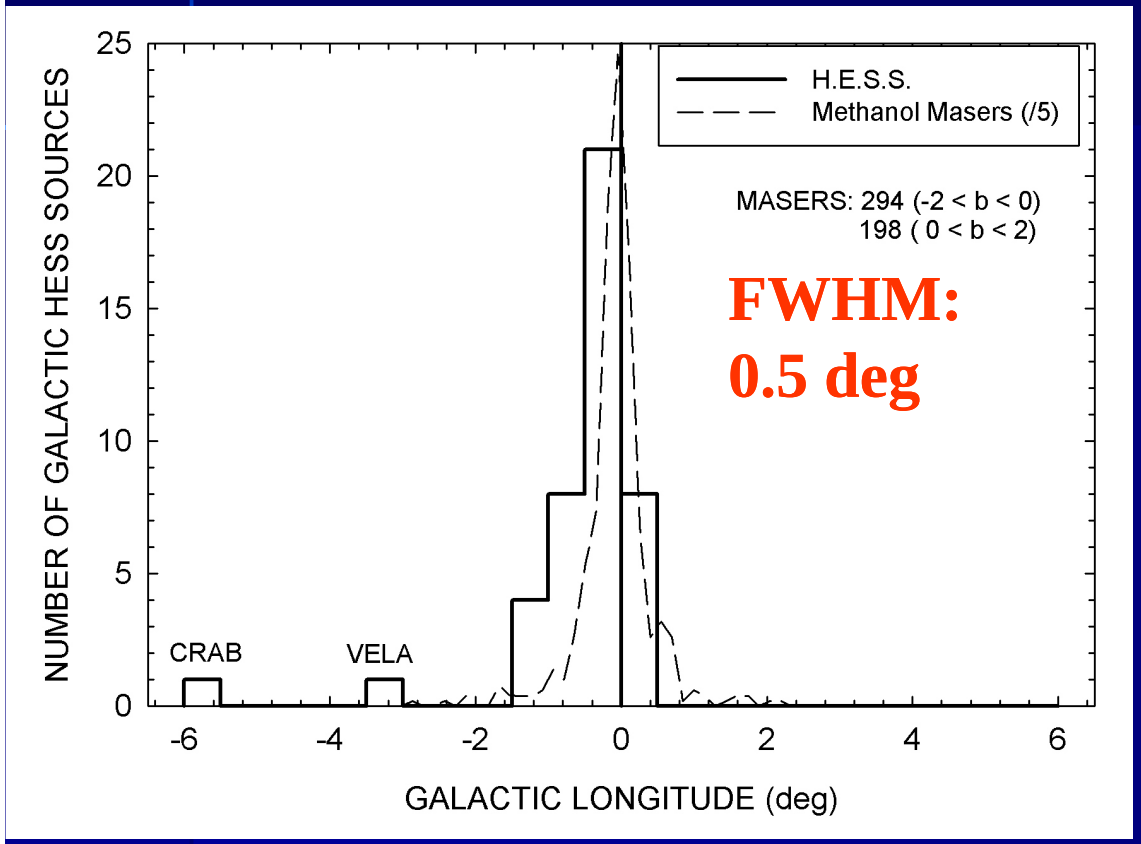

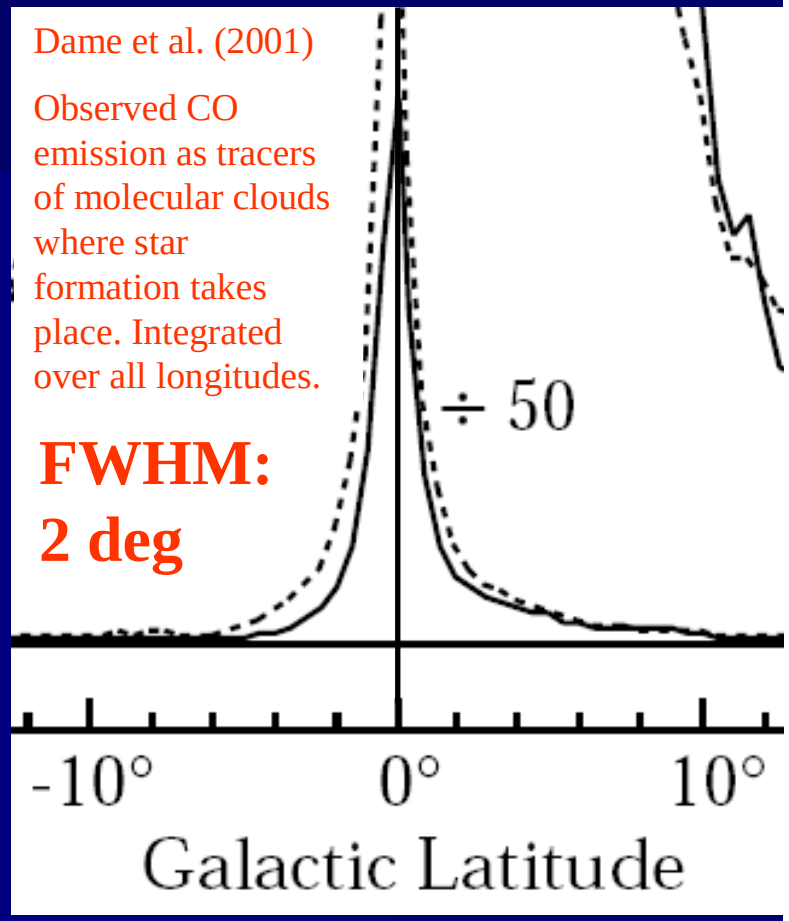

SNR Explosion in Anisotropic Media

Blondin et al. (2001); Ferreira & de Jager (2008)

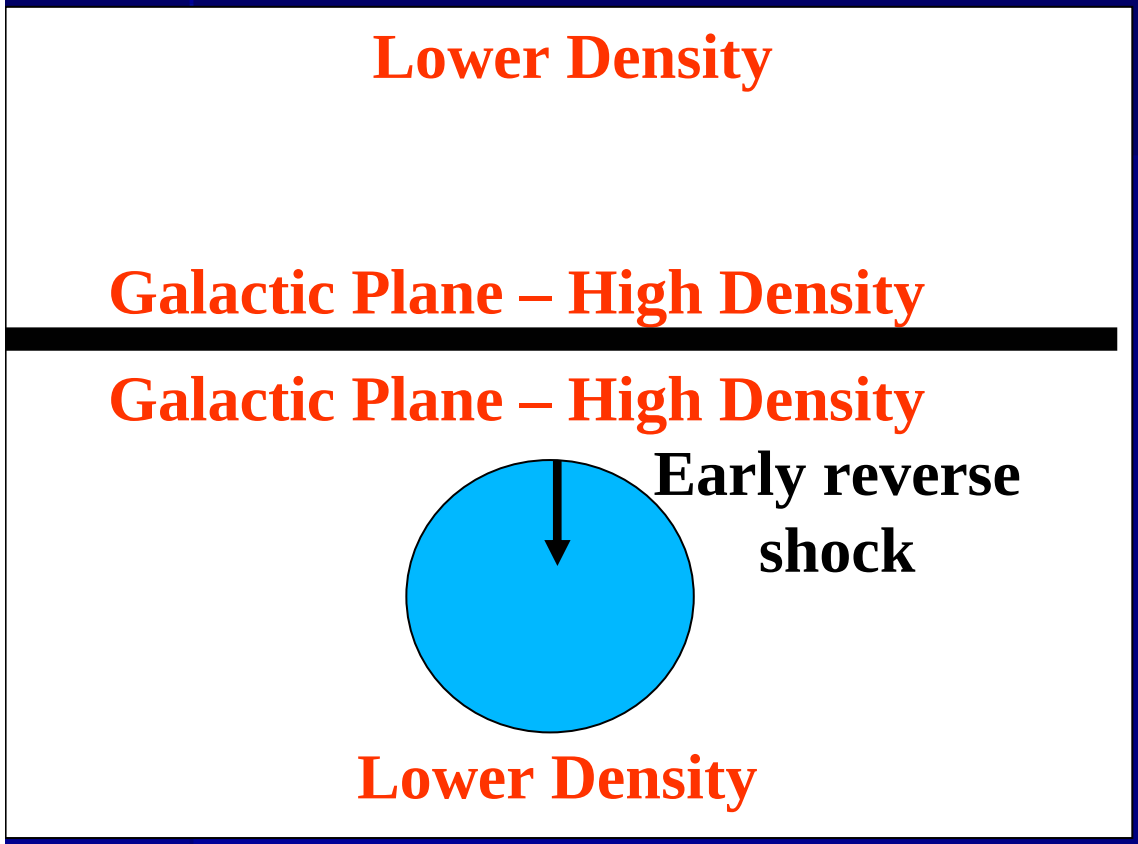

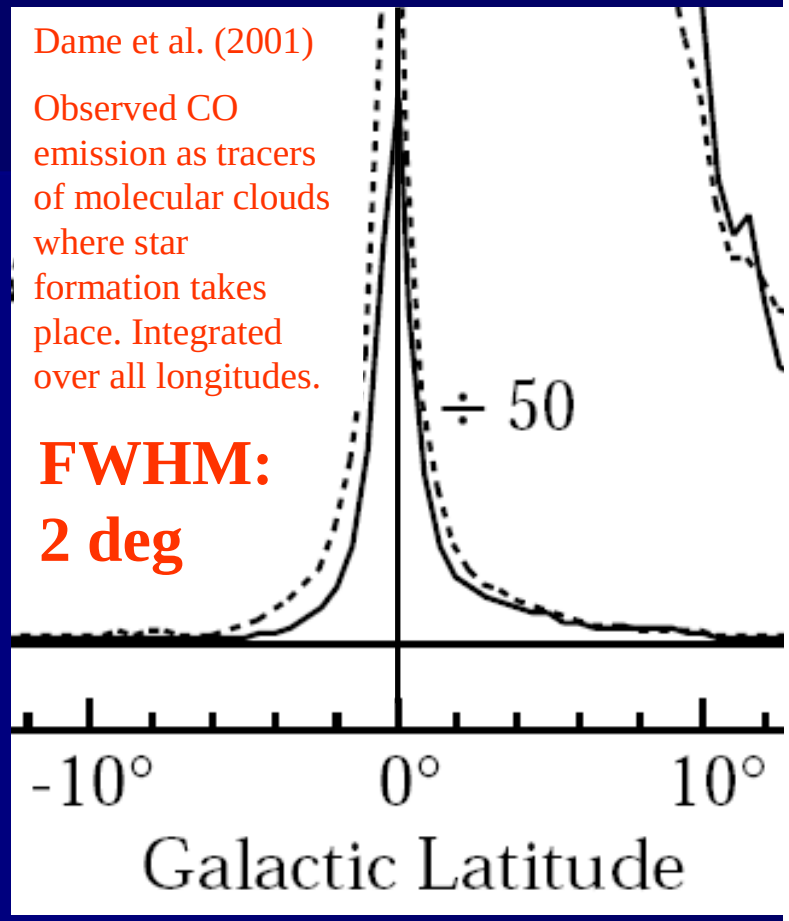

SNR Explosion in Anisotropic Media

Lower Density

Galactic Plane – High Density

Galactic Plane – High Density

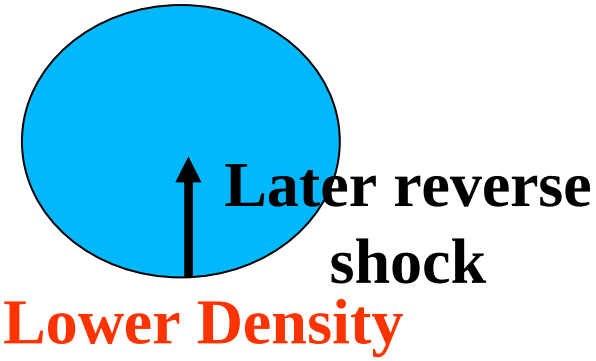

Ferreira & de Jager (2008)

The return time of the Reverse Shock scales with ISM density as

$T_R \sim (\text{density})^{-1/3}$.

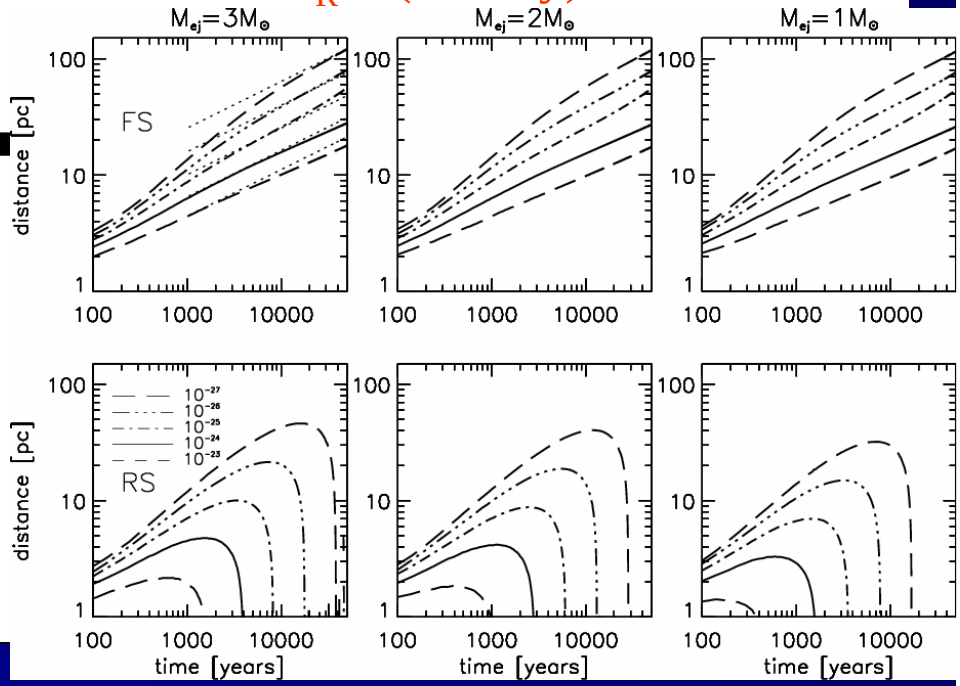

$$t_R = 4000\left(\frac{\rho_{ISM}}{\rho_0}\right)^{-1/3}\left(\frac{M_{ej}}{M_0}\right)^{3/4}\left(\frac{E_{ej}}{E_0}\right)^{-45/100}\left(\frac{\gamma}{\gamma_0}\right)^{-3/2} y.$$

PWNe Offset from Pulsars

de Jager & Djannati-Atai (2008); Hessels et al. (2008)

Table 1. HESS VHE γ-ray Sources Possibly Associated with PWNe

HESS Source	Size[a] (arcmin)	Pulsar / PWN	Offset (arcmin)	P_{spin} (ms)	τ_c (kyr)	$\dot{E}$ $\times 10^{36}$ (ergs s^{-1})	d[b] (kpc)	$L_\gamma/\dot{E}$ (1 − 10 TeV) (%)	Assoc. Ref.
J0534+220	...	B0531+21	...	33	1	460	2	0.009	1
J0835−455	26	B0833−45	18	89	11	6.9	0.3	0.008	2
J0852−463	60	J0855−4644	43	65	141	1.1	*2*	3	3
J1303−631	10	J1301−6305	11	185	11	1.7	*7*	5	4
J1418−609[c]	4	G313.3+0.1	8	...	...	...	...	...	5
J1420−607	4	J1420−6048	3	68	13	10	*6*	0.4	5
J1514−591	6	B1509−58	2	151	16	18	*4*	0.2	6
J1616−508	8	J1617−5055	10	69	8	16	*7*	0.6	7
J1640−465	3	G338.3−0.0	...	...	...	...	...	...	8
J1702−420	18	J1702−4128	35	182	55	0.34	*5*	5	9
J1718−385	9	J1718−3825	8	75	90	1.3	*4*	0.4	10
J1747−281	...	G0.9+0.1	...	...	...	...	...	...	11
J1804−216	12	B1800−21	10	134	16	2.2	*4*	2	12
J1809−193	32	J1809−1917	12	83	51	1.8	*4*	1	13
J1813−178	2	G12.8−0.0	...	...	...	...	...	...	14
J1825−137	10	B1823−13	11	101	21	2.8	*4*	1	15
J1833−105	...	J1833−1034	...	62	5	34	*3*	0.008	16
J1837−069	7	J1838−0655	6	70	23	5.5	7	1	17
J1846−029	...	J1846−0258	...	326	1	8.1	6	0.1	16
J1857+026	7	J1856+0245	8	81	21	4.6	*9*	3	18
J1912+101	16	J1913+1011	9	36	170	2.9	*5*	0.6	19

PWNe Offset from Pulsars

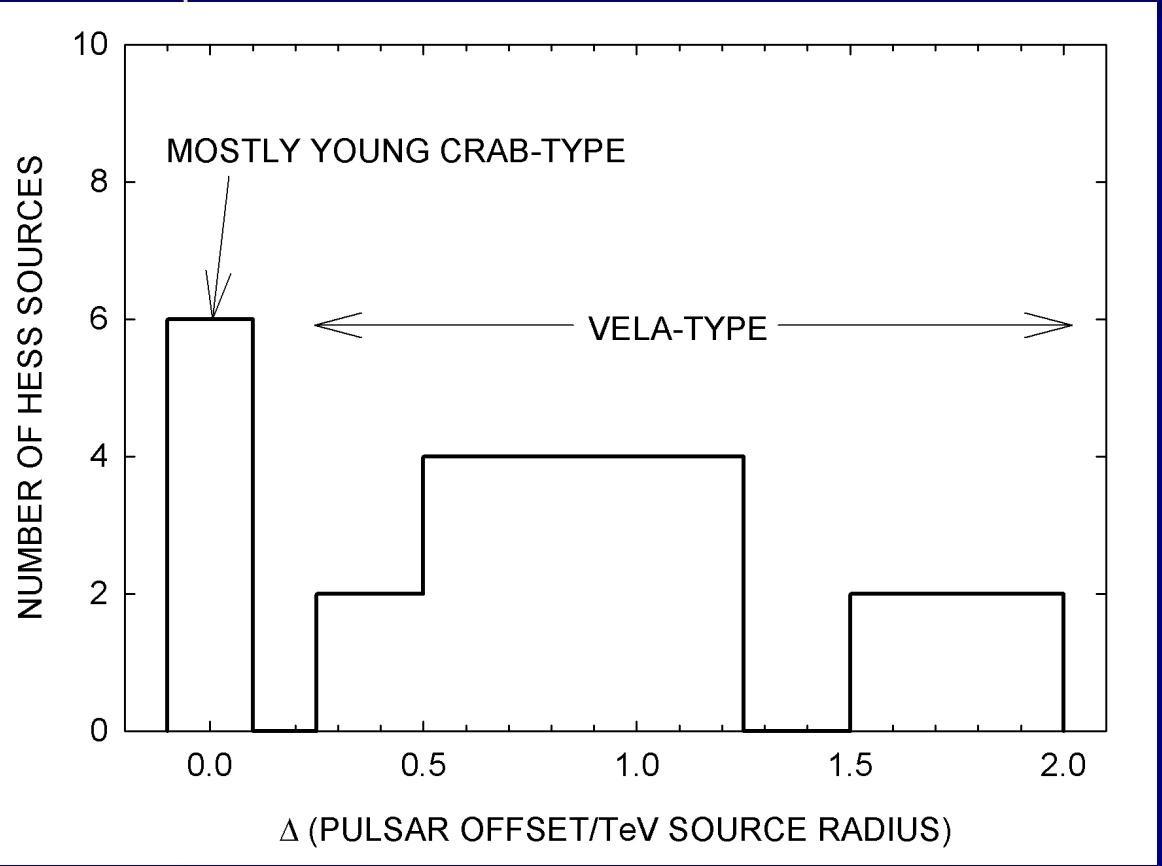

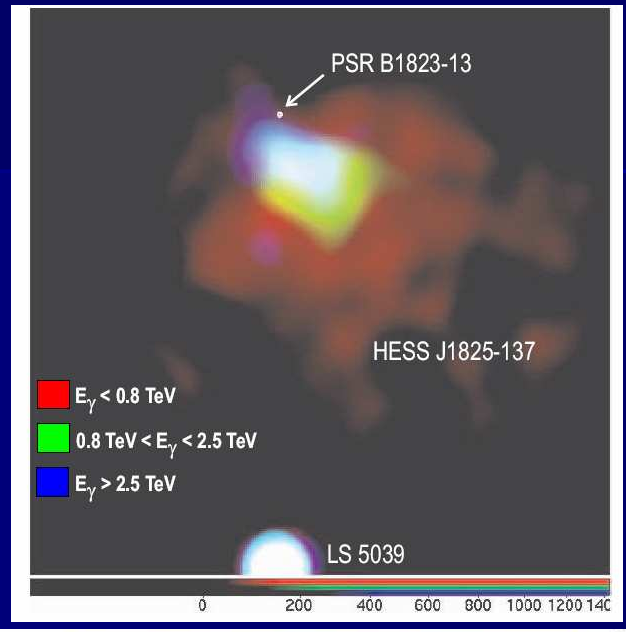

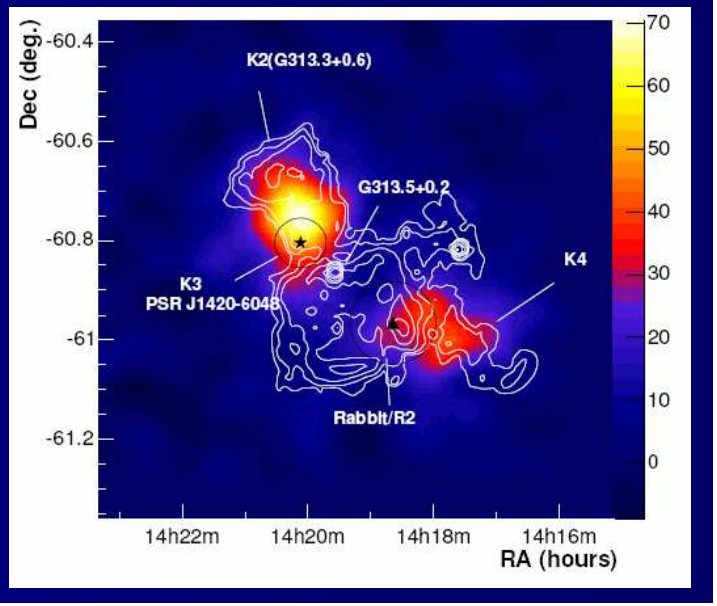

Photon Index Distribution
The X-ray connection

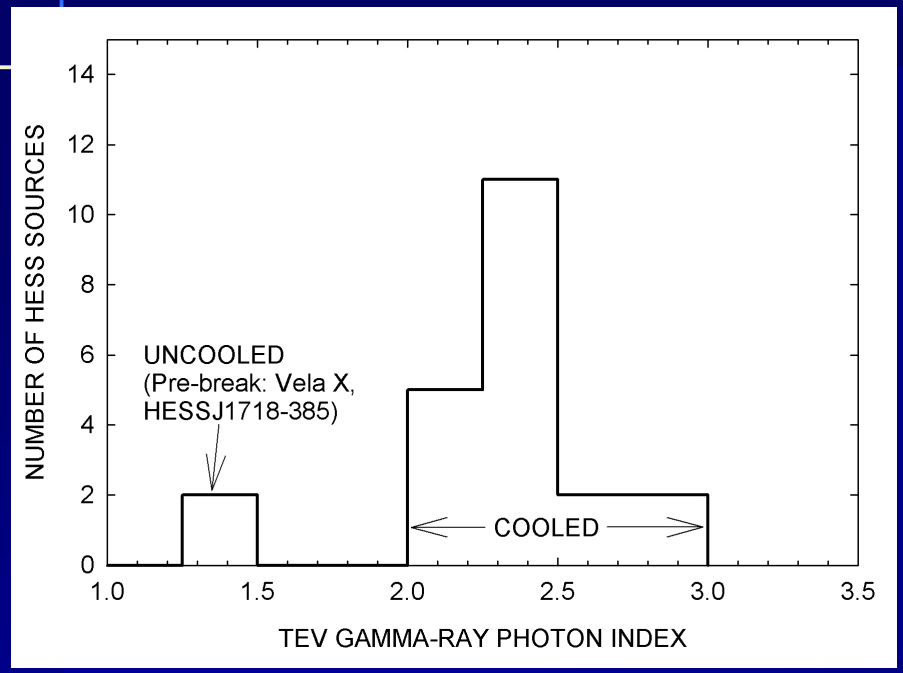

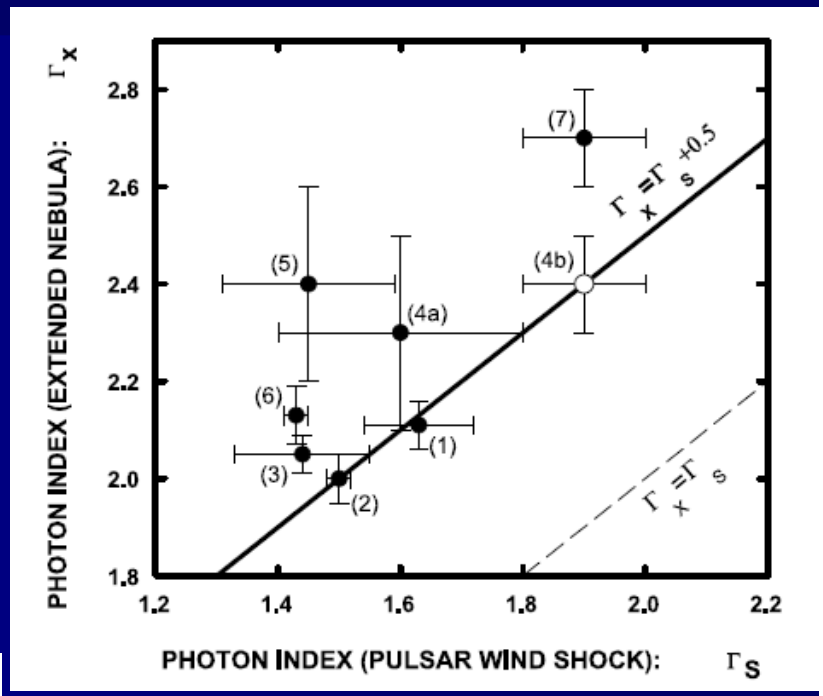

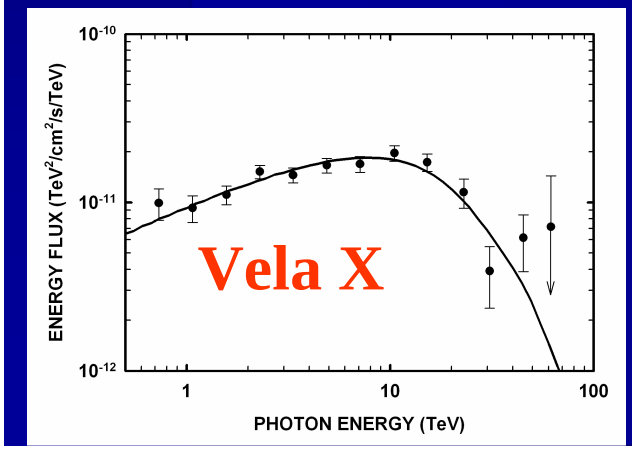

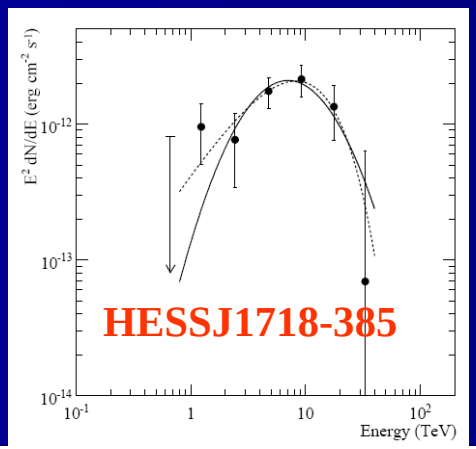

Numerical Scheme for SNR and PWN

(see Chevalier (2005) for analytical approach)

Euler equations

$$\frac{\partial}{\partial t}\rho + \nabla \cdot (\rho \mathbf{v}) = 0,$$

$$\frac{\partial}{\partial t}(\rho \mathbf{v}) + \nabla \cdot (\rho \mathbf{v}\mathbf{v} + P\mathbf{I}) = 0,$$

$$\frac{\partial}{\partial t}\left(\frac{\rho}{2}\mathbf{v}^2 + \frac{P}{\gamma - 1}\right) + \nabla \cdot \left(\frac{\rho}{2}\mathbf{v}^2\mathbf{v} + \frac{\gamma \mathbf{v} P}{\gamma - 1}\right) = 0$$

For the initial and boundary conditions of the SNR

$$v = \frac{r}{t} = v_{ej} r / r_{ej}.$$

$$v_{ej} = \sqrt{\frac{10}{3}\frac{E_{ej}}{M_{ej}}}.$$

$$\rho_{ej} = \frac{3M_{ej}}{4\pi r_{ej}^3}$$

$r_{ej} = 0.1$ pc

adiabatic index of 5/3

For the PWN we allow input power to decrease as a dipole spinning down. Magnetic field generation in PWN according to Faraday induction. Not fully MHD since field is calculated kinematically from flow (Scherer & Ferreira 2005).

$$L(t) = \frac{L_0}{\left(1 + \frac{t}{\tau}\right)^2}$$

$$\frac{\partial \mathbf{B}}{\partial t} + \nabla \times (\mathbf{v} \times \mathbf{B}) = 0$$

Numerical scheme of LeVeque (2002), Ferreira & de Jager (2008), using wave propagation approach to solve hyperbolic differential equations. See also van der Swaluw et al. (2001), Bucciantini et al. (2003). One fluid approach since post shocked flow downstream is non-relativistic v<c/3 (van der Swaluw et al. (2001).

Evolutionary radiation model, constrained by MHD results.

Two-component (radio/X-ray) injection (Venter & de Jager 2006)

$$Q(\gamma,t) = \begin{pmatrix} Q_0(t)(\gamma/\gamma_b)^{-p_1} \text{ for } \gamma < \gamma_b \\ Q_0(t)(\gamma/\gamma_b)^{-p_2} \text{ for } \gamma_b < \gamma < \gamma_{\max} \end{pmatrix} \quad \int Q(\gamma,t)\gamma d\gamma = \eta L(t).$$

L(0) (or P_0) constrained by R_{PWN}/R_{SNR} from MHD

Particle spectrum from Leaky Box approach:
see e.g. Zhang et al. (2008)

$$\frac{dN(E_e,\ T_{\rm age})}{dE_e} = \int_0^{T_{\rm age}} Q(E_e,t)\exp\left(-\frac{T_{\rm age}-t}{\tau_{\rm eff}}\right)dt$$

Effective loss timescales constrained by MHD

Pair production multiplicity from continuity equation (Sefako & de Jager 2003)

The electron continuity equation is given by

$$\int_0^\infty Q(E)\,dE = \eta_p \frac{I_{\rm GJ} M}{e}\,, \qquad (3)$$

where η_p is the fraction of all pairs escaping through the light cylinder, which contributes to the compact nebular emission. The expression for the Goldreich-Julian current (converted to a rate) from the pulsar polar caps is $I_{\rm GJ}/e \sim (6\dot{E}c)^{1/2}/e$. The pair-creation multiplicity is M, as defined earlier.

Maximum particle energy constrained by gyroradius limit ($\varepsilon = r_g/R_s$). PWN termination shock radius cancels out (Venter & de Jager 2006; de Jager & Djannati-Atai 2008)

$$E_{\max}(t) \approx \frac{e}{2}\sqrt{\frac{\sigma L(t)}{(1+\sigma)c}}$$

$$= (110\,\text{TeV})\kappa\left(\frac{\epsilon}{0.2}\right)\left(\frac{\sigma}{0.1}\dot{E}_{36}\right)^{1/2}$$

Adding the effect of birth & braking index

Evolution of average field strength

(Ferreira & de Jager, 2008, A&A subm)

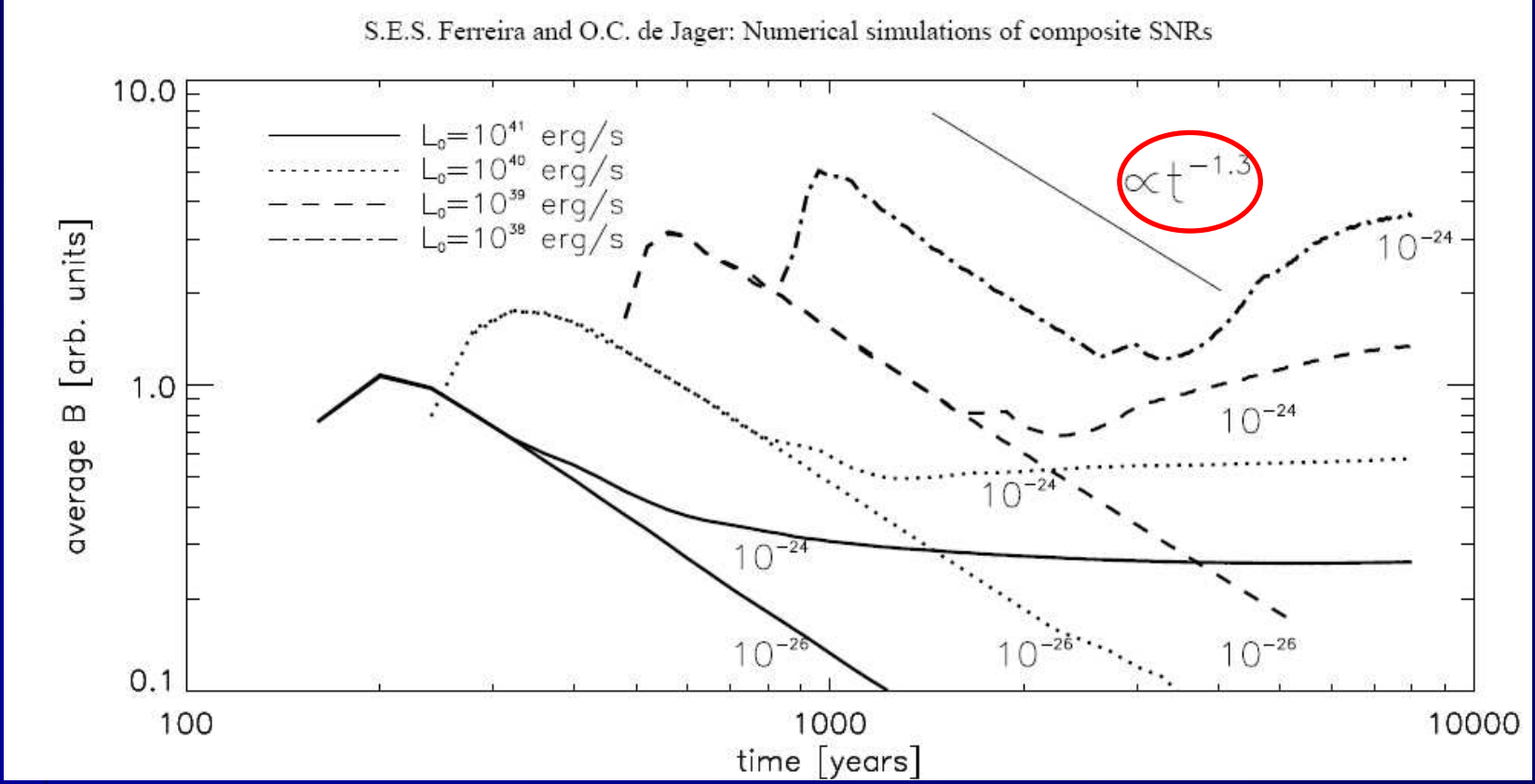

G21.5-0.9

- $L = 4.7 \times 10^{37}$ erg/s
- R_{PWN}=1.2 pc; R_{SNR}=3.3 pc
- Expansion age 870 ± 200 yr => P_0=55 ms given P=61.8 ms.
- $\int(-\dot{E})dt \approx 3.8 \times 10^{48}$ erg for $L_0=1.1\times10^{38}$ erg/s.
- Requires $n \approx 0.6$ cm^{-3} to reproduce R_{SNR}=3.3 pc after a kyr.
- Requires $8M_o$ ejecta mass to reproduce R_{PWN} radius.
- Equipartition argument gives $E_{min} \approx 3.2\times10^{47}$ erg (Bocchino et al. 2005) and B_{eq}=0.2 mG.
- H.E.S.S. observations give lower field strength (Djannati-Atai et al. 2007) $B \approx 25\ \mu G$ => ten times lower than equiparition.

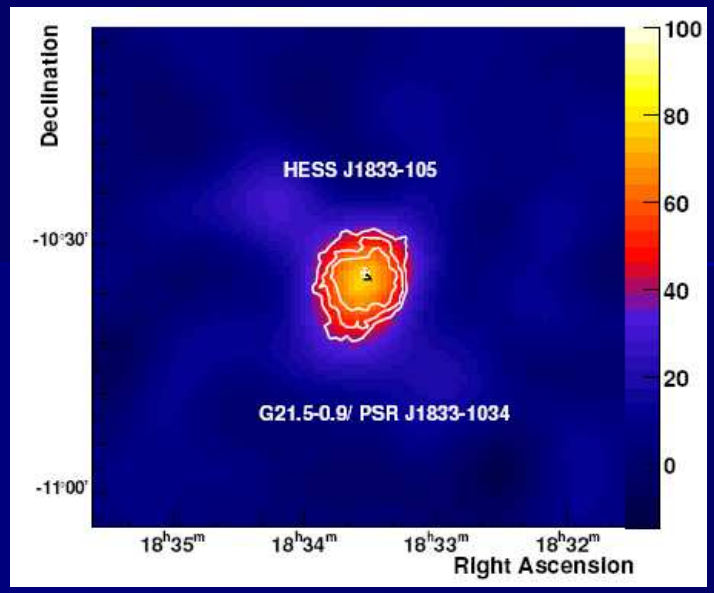

H.E.S.S.: Djannati-Ataï et al. (2007)

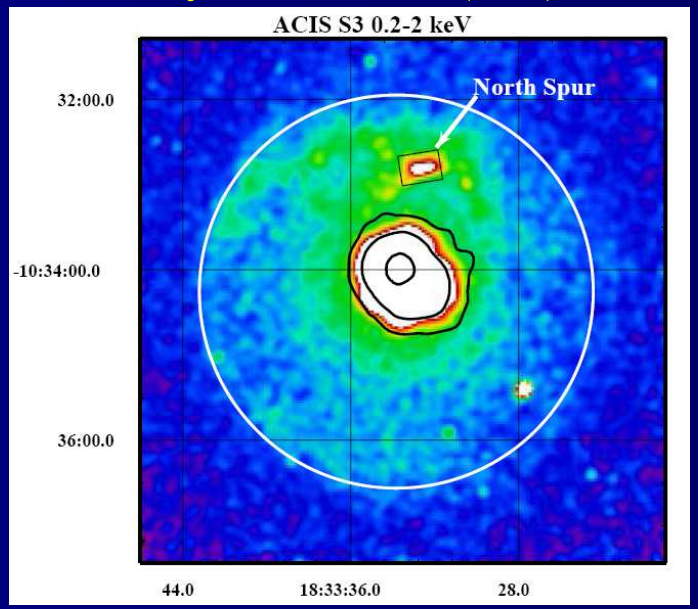

XMM-Newton: Bocchino et al. (2005)

EVOLUTION MEAN FIELD STRENGTH IN PWN of G21.5-0.9

($L_0 = 10^{38}$ erg/s; τ = 3000 yr; $M_{ej} = 8M_o$; $n_{ISM} = 0.6$ cm^{-3})

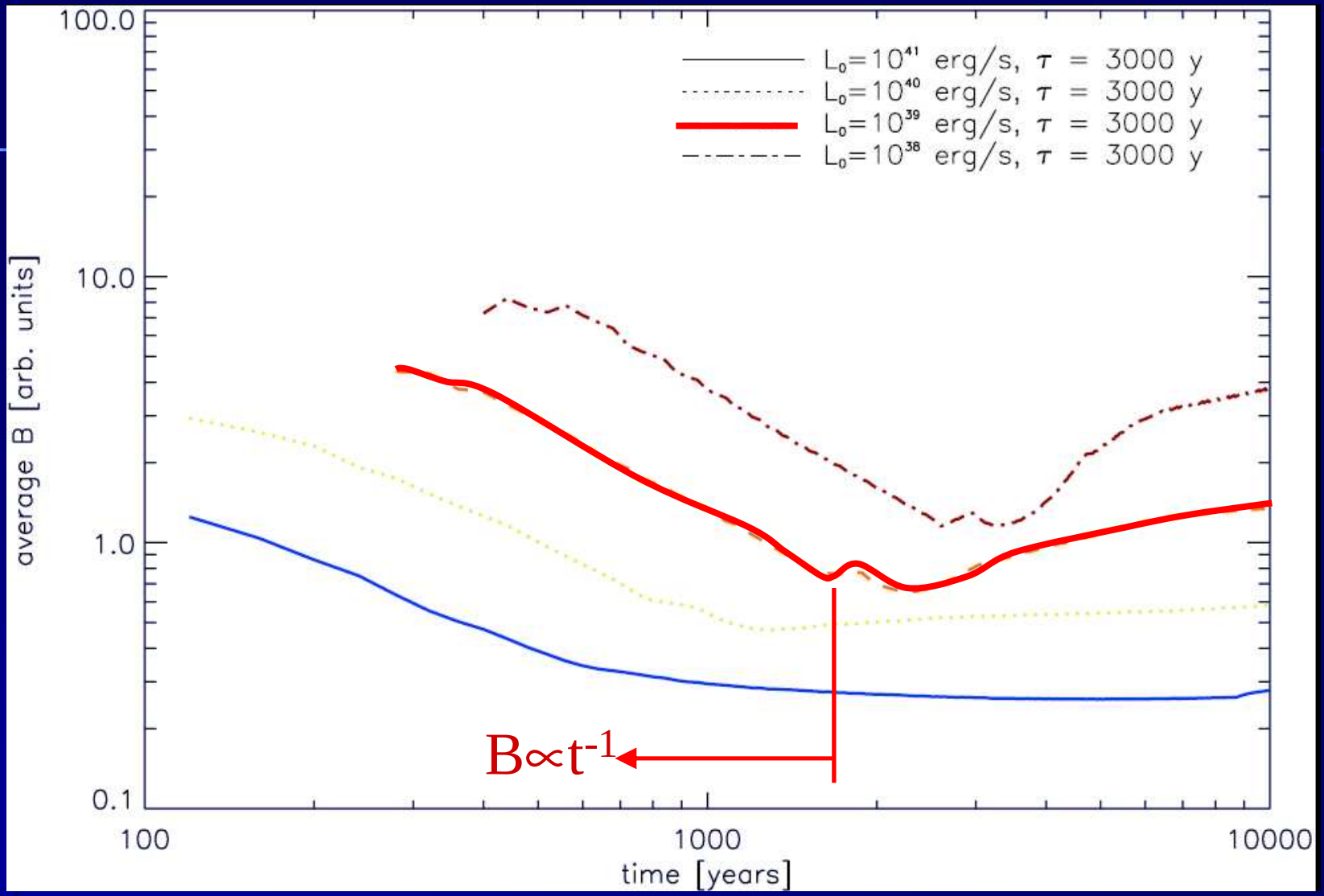

RADIATION SPECTRUM OF G21.5-0.9

B=25 μG (T/t); 70% Conversion Efficiency

However, Birth Period and Efficiency are correlated, but Birth Period and Age is also correlated!

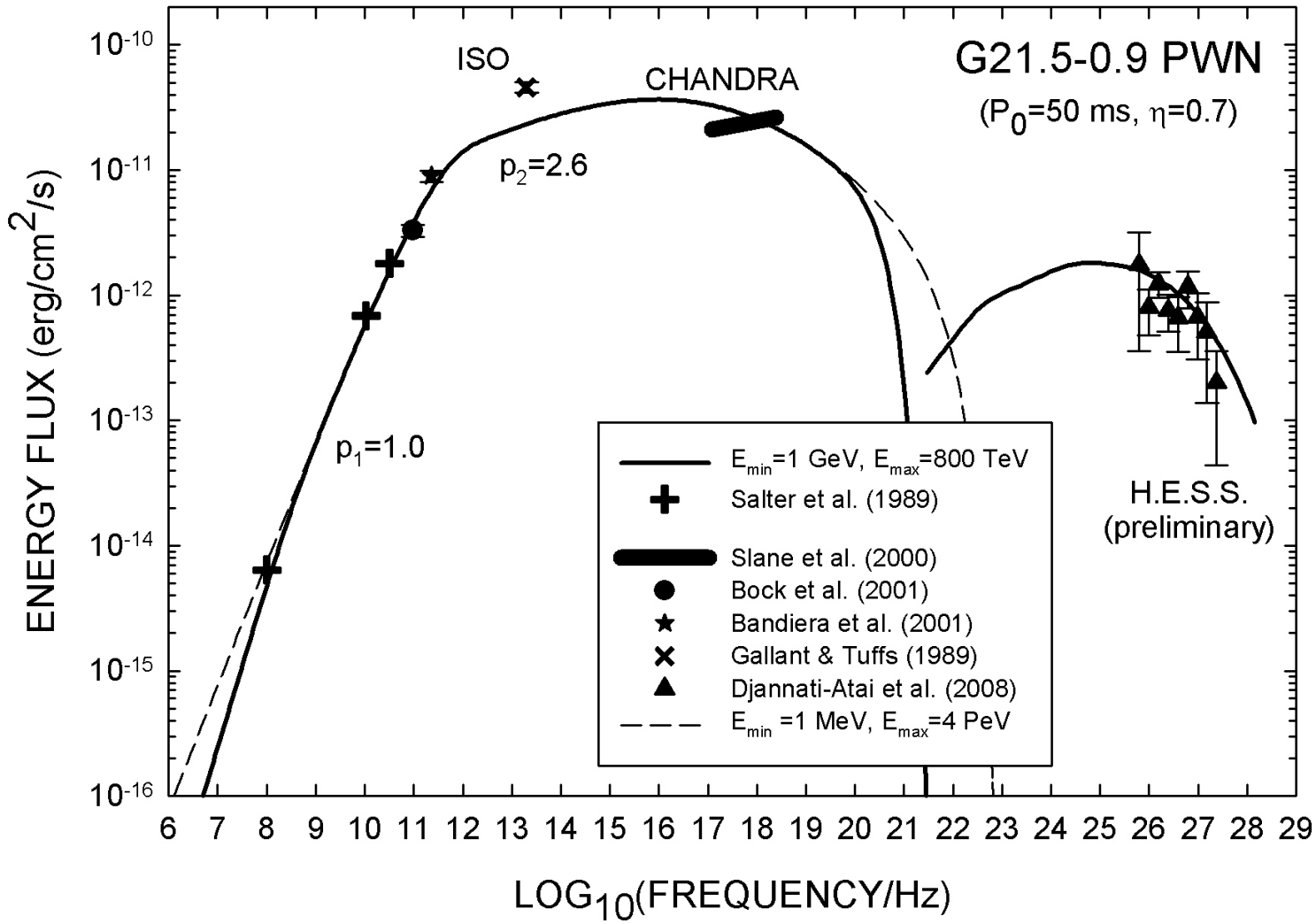

G21.5-0.9

- Pair production multiplicity:
  $2.2 \times 10^5 > M > 0.9 \times 10^5$
- Challenge for standard models?

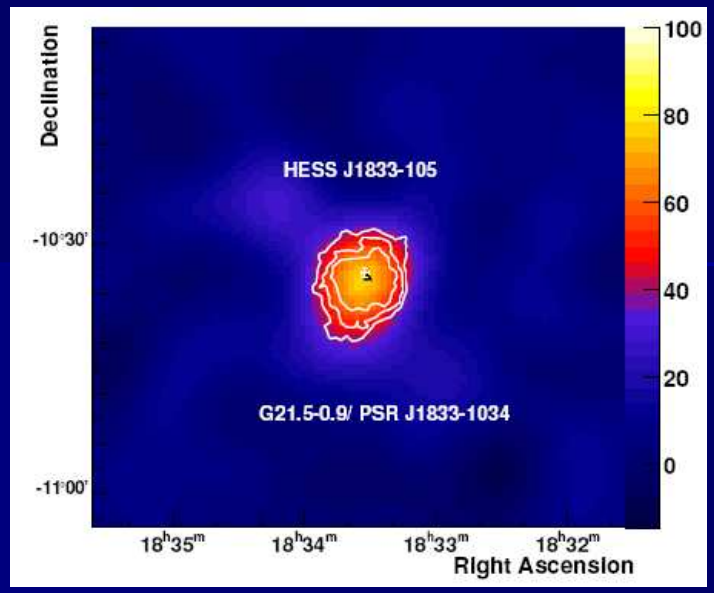

H.E.S.S.: Djannati-Ataï et al. (2007)

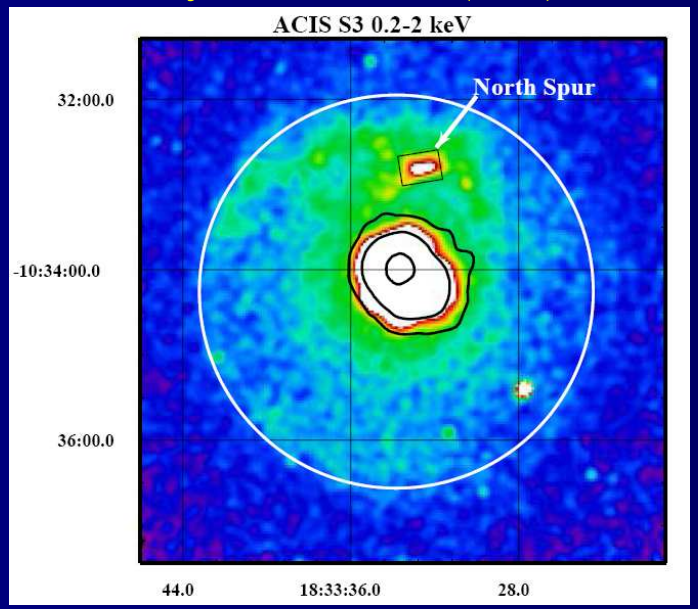

XMM-Newton: Bocchino et al. (2005)

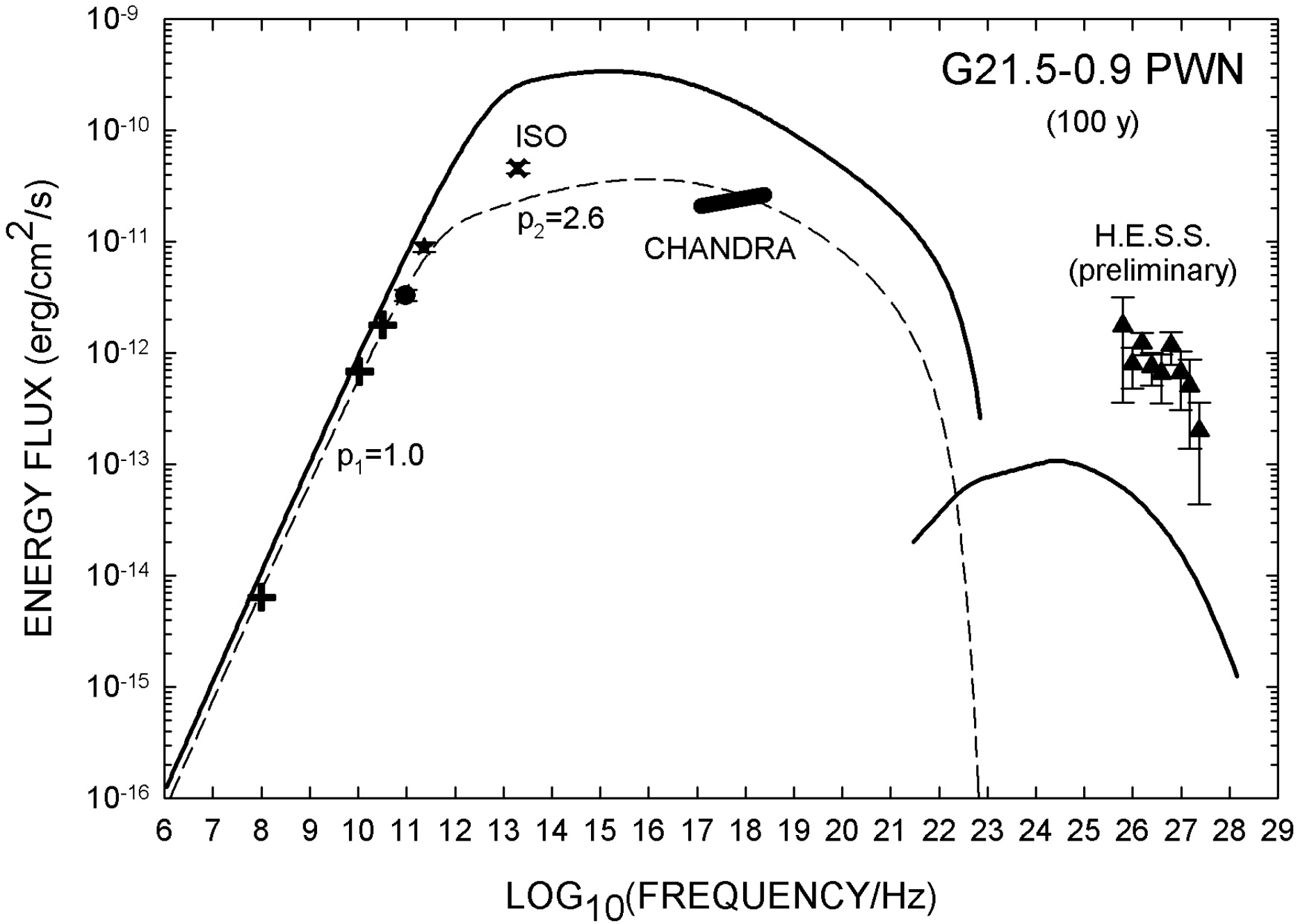
G21.5-0.9 PWN
(100 y)
ISO
p_2=2.6
CHANDRA
H.E.S.S.
(preliminary)
p_1=1.0
ENERGY FLUX (erg/cm^2/s)
LOG$_{10}$(FREQUENCY/Hz)
10^{-9}
10^{-10}
10^{-11}
10^{-12}
10^{-13}
10^{-14}
10^{-15}
10^{-16}
6 7 8 9 10 11 12 13 14 15 16 17 18 19 20 21 22 23 24 25 26 27 28 29

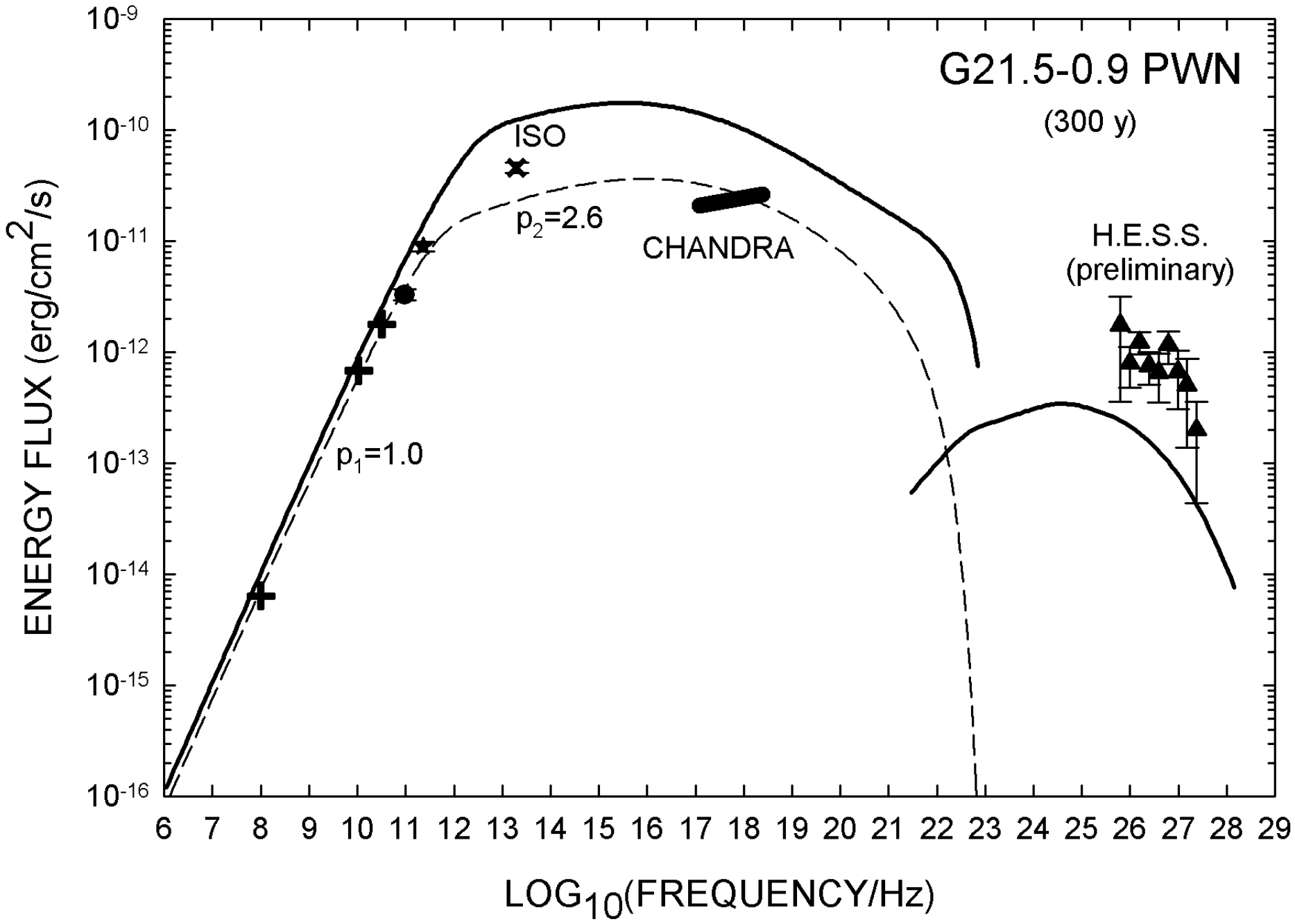
G21.5-0.9 PWN
(300 y)
ISO
p_2=2.6
CHANDRA
H.E.S.S.
(preliminary)
p_1=1.0
ENERGY FLUX (erg/cm^2/s)
LOG$_{10}$(FREQUENCY/Hz)
10^{-9}
10^{-10}
10^{-11}
10^{-12}
10^{-13}
10^{-14}
10^{-15}
10^{-16}
6 7 8 9 10 11 12 13 14 15 16 17 18 19 20 21 22 23 24 25 26 27 28 29

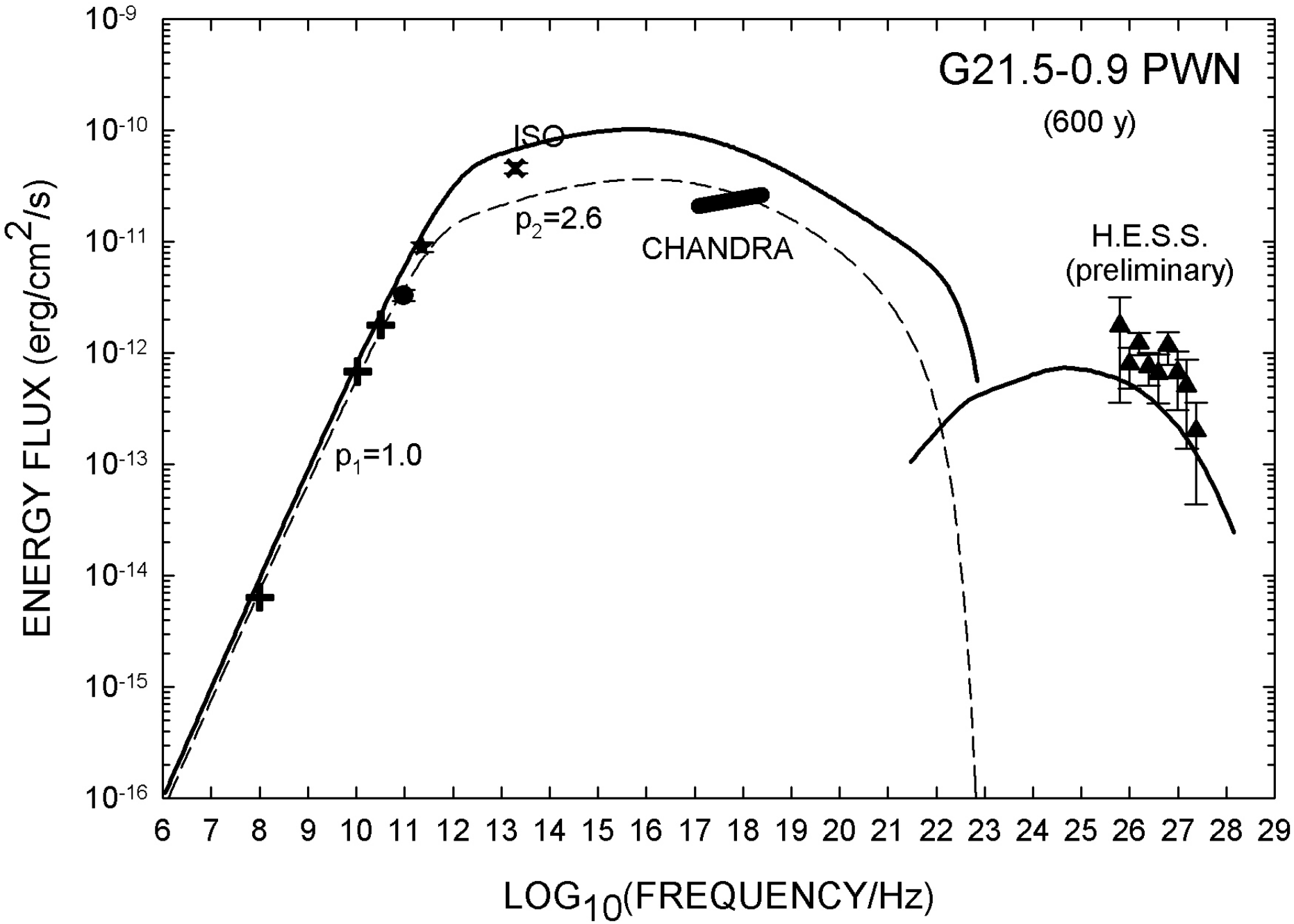
G21.5-0.9 PWN
(600 y)
ISO
p_2=2.6
CHANDRA
H.E.S.S.
(preliminary)
p_1=1.0
ENERGY FLUX (erg/cm^2/s)
LOG$_{10}$(FREQUENCY/Hz)
10^{-9}
10^{-10}
10^{-11}
10^{-12}
10^{-13}
10^{-14}
10^{-15}
10^{-16}
6 7 8 9 10 11 12 13 14 15 16 17 18 19 20 21 22 23 24 25 26 27 28 29

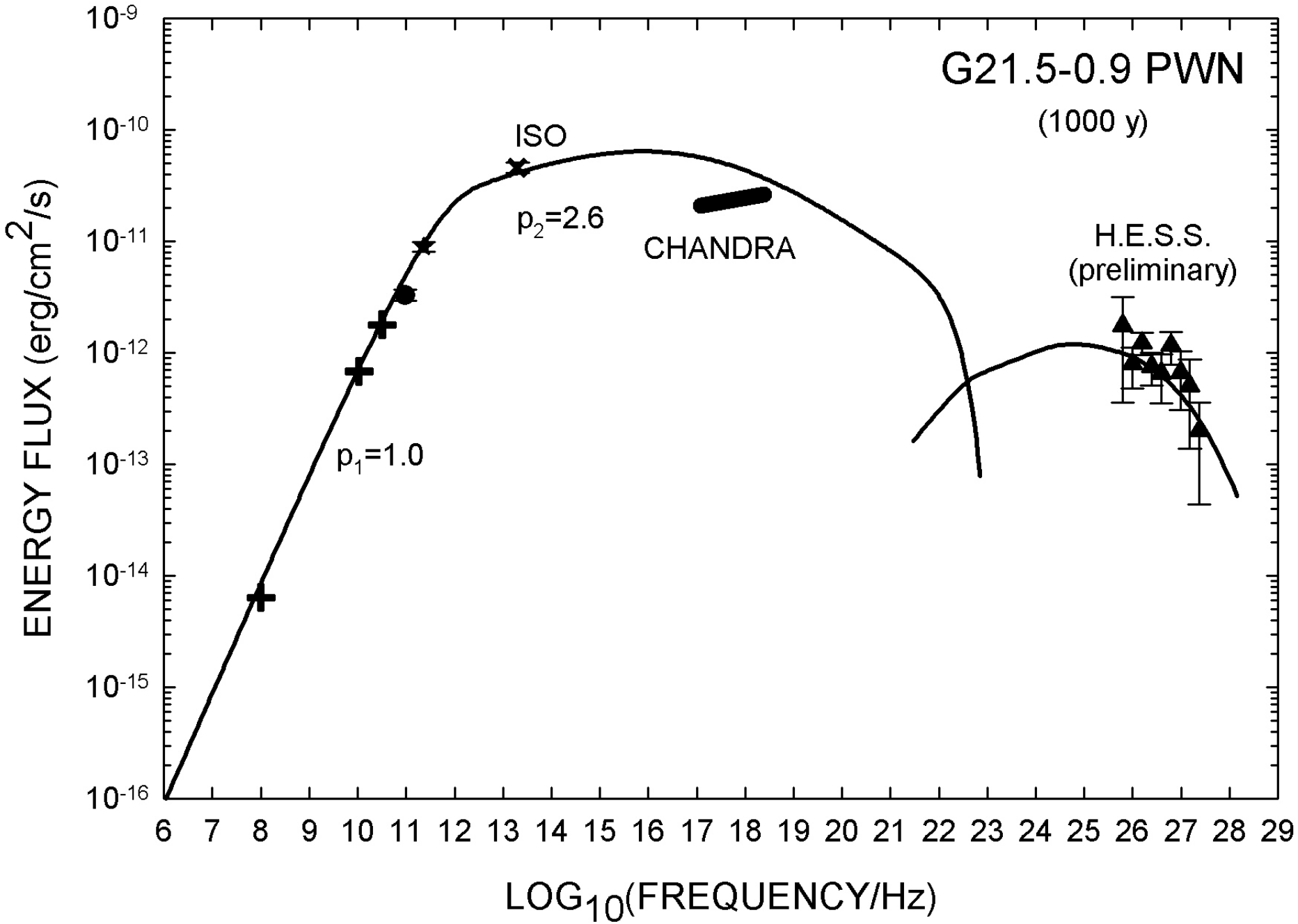
G21.5-0.9 PWN
(1000 y)
ISO
p_2=2.6
CHANDRA
H.E.S.S.
(preliminary)
p_1=1.0
ENERGY FLUX (erg/cm^2/s)
10^{-9}
10^{-10}
10^{-11}
10^{-12}
10^{-13}
10^{-14}
10^{-15}
10^{-16}
6 7 8 9 10 11 12 13 14 15 16 17 18 19 20 21 22 23 24 25 26 27 28 29
LOG$_{10}$(FREQUENCY/Hz)

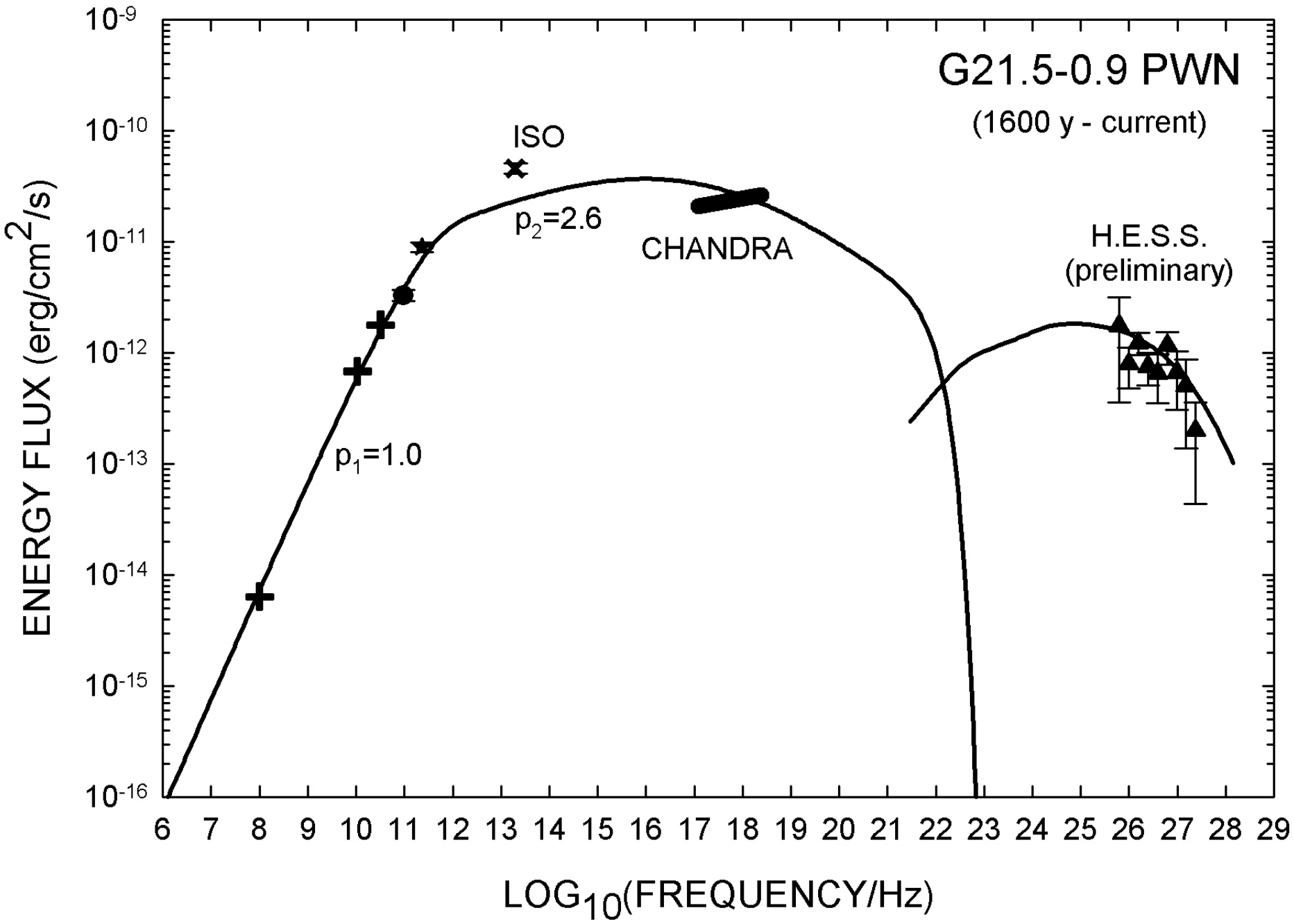
G21.5-0.9 PWN
(1600 y - current)
ISO
p_2=2.6
CHANDRA
H.E.S.S.
(preliminary)
p_1=1.0
ENERGY FLUX (erg/cm^2/s)
LOG$_{10}$(FREQUENCY/Hz)
10^{-9}
10^{-10}
10^{-11}
10^{-12}
10^{-13}
10^{-14}
10^{-15}
10^{-16}
6 7 8 9 10 11 12 13 14 15 16 17 18 19 20 21 22 23 24 25 26 27 28 29

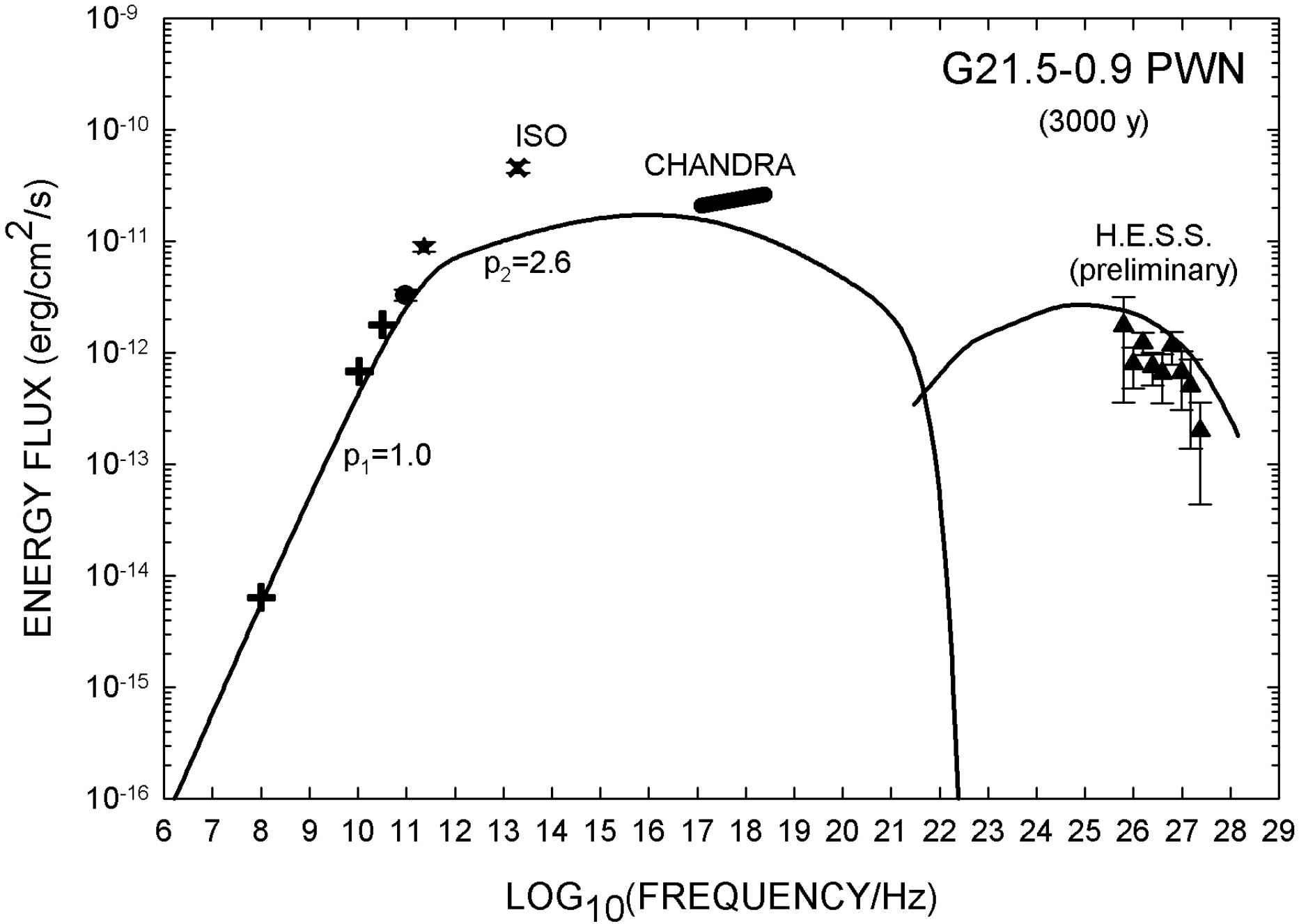
G21.5-0.9 PWN
(3000 y)
ISO
CHANDRA
H.E.S.S.
(preliminary)
p_2=2.6
p_1=1.0
ENERGY FLUX (erg/cm^2/s)
LOG$_{10}$(FREQUENCY/Hz)
10^{-9}
10^{-10}
10^{-11}
10^{-12}
10^{-13}
10^{-14}
10^{-15}
10^{-16}
6 7 8 9 10 11 12 13 14 15 16 17 18 19 20 21 22 23 24 25 26 27 28 29

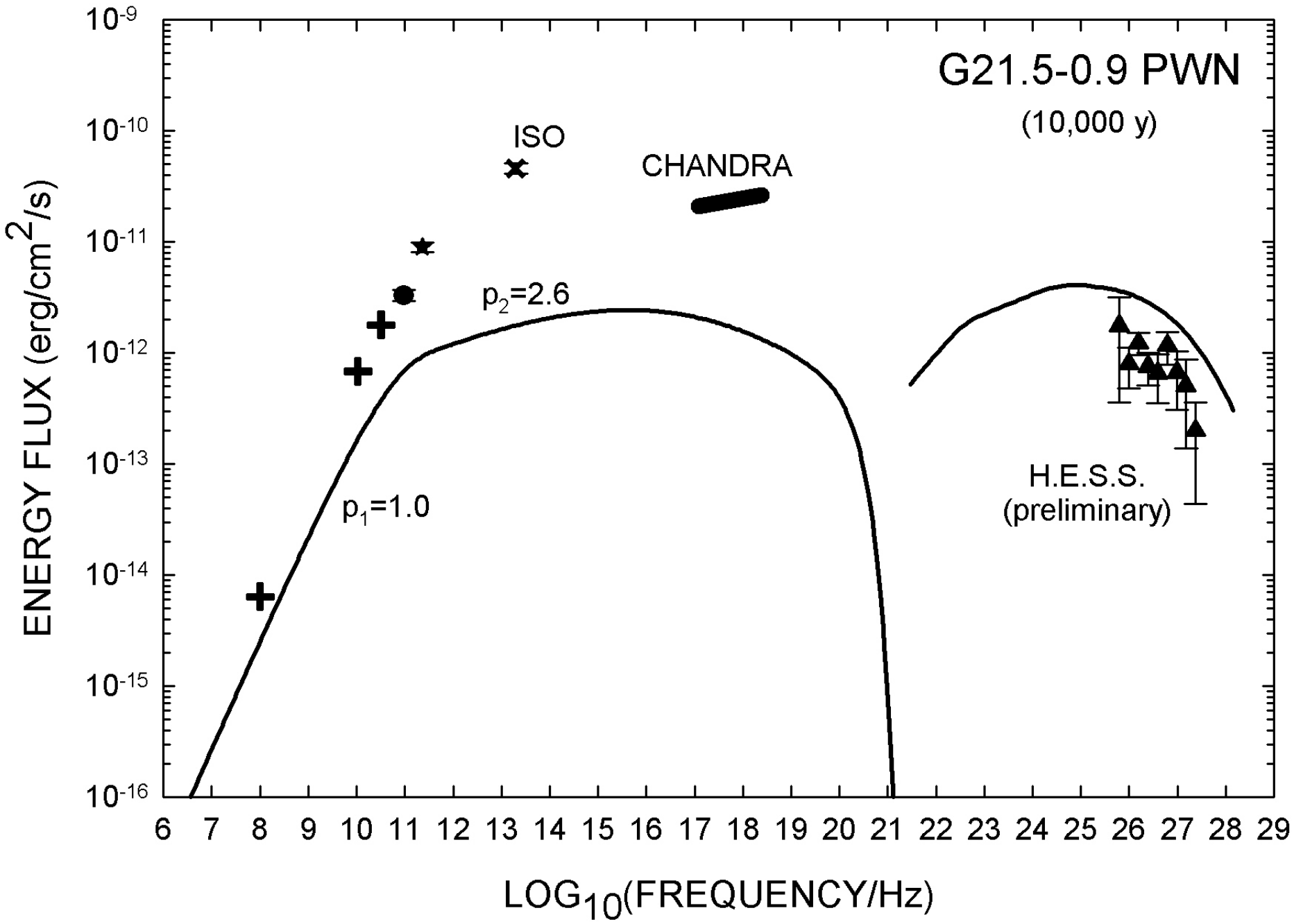
G21.5-0.9 PWN
(10,000 y)
ISO
CHANDRA
p_2=2.6
p_1=1.0
H.E.S.S.
(preliminary)
ENERGY FLUX (erg/cm^2/s)
LOG$_{10}$(FREQUENCY/Hz)
10^{-9}
10^{-10}
10^{-11}
10^{-12}
10^{-13}
10^{-14}
10^{-15}
10^{-16}
6 7 8 9 10 11 12 13 14 15 16 17 18 19 20 21 22 23 24 25 26 27 28 29

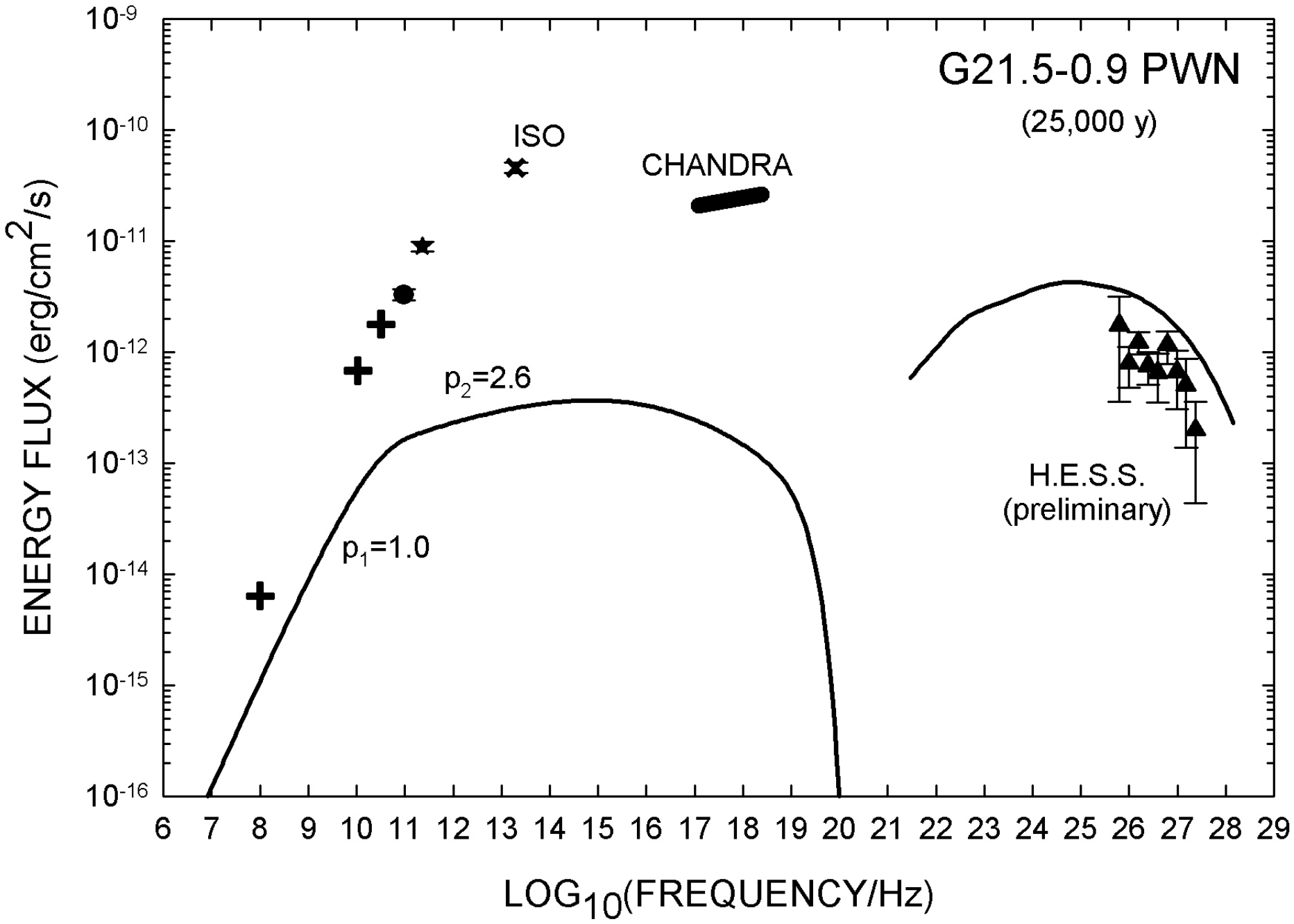
G21.5-0.9 PWN
(25,000 y)
ISO
CHANDRA
p_2=2.6
p_1=1.0
H.E.S.S.
(preliminary)
ENERGY FLUX (erg/cm^2/s)
LOG$_{10}$(FREQUENCY/Hz)
10^{-9}
10^{-10}
10^{-11}
10^{-12}
10^{-13}
10^{-14}
10^{-15}
10^{-16}
6 7 8 9 10 11 12 13 14 15 16 17 18 19 20 21 22 23 24 25 26 27 28 29

Evolutionary parameters for SNR expansion into ISM with low density .

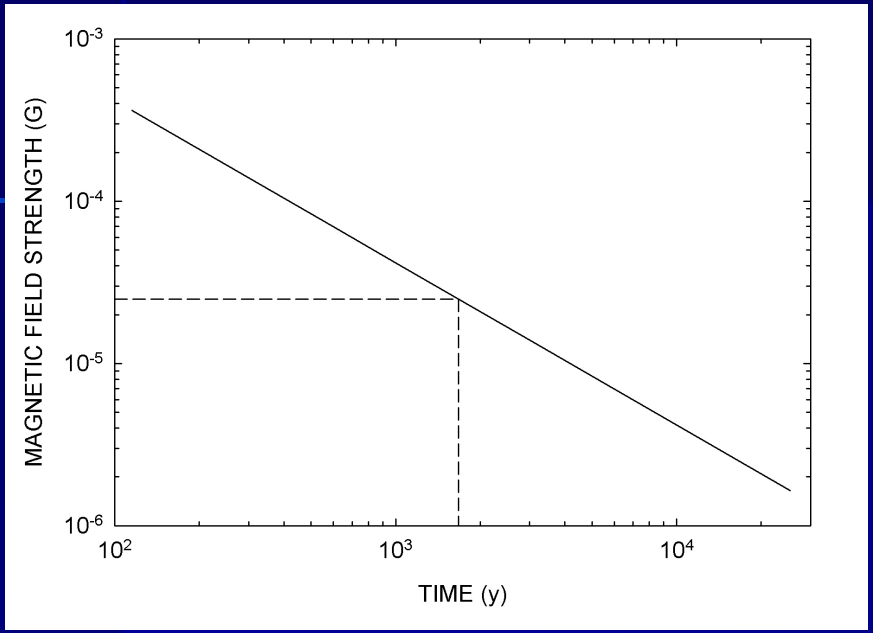

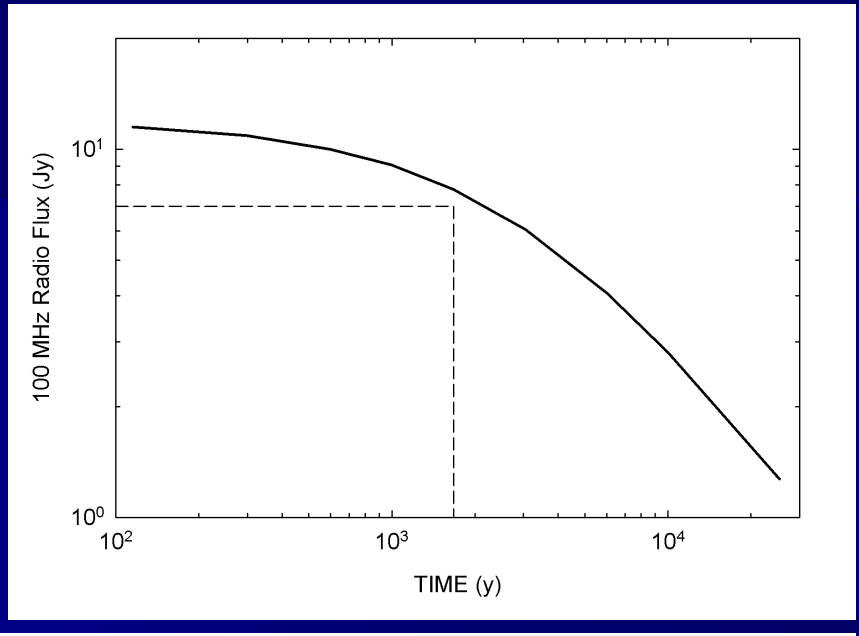

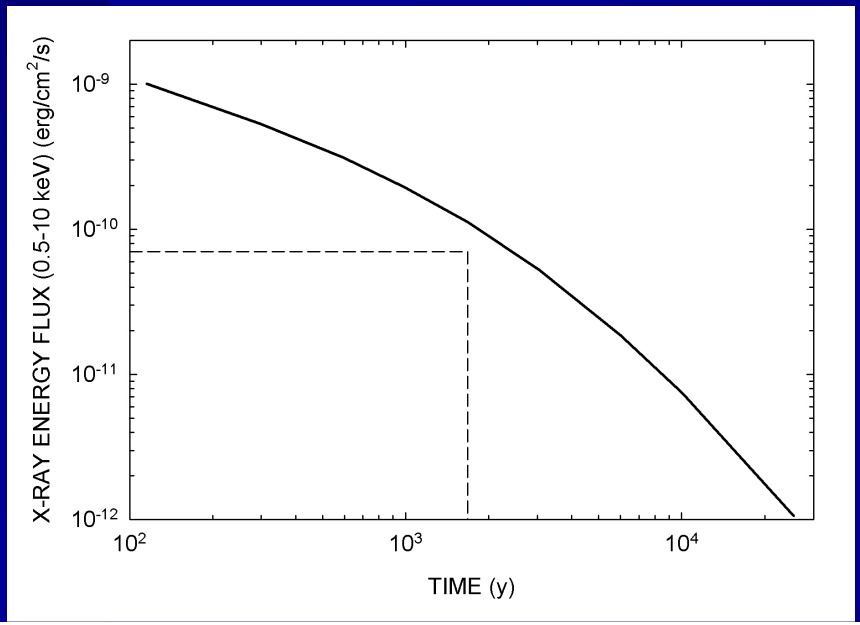

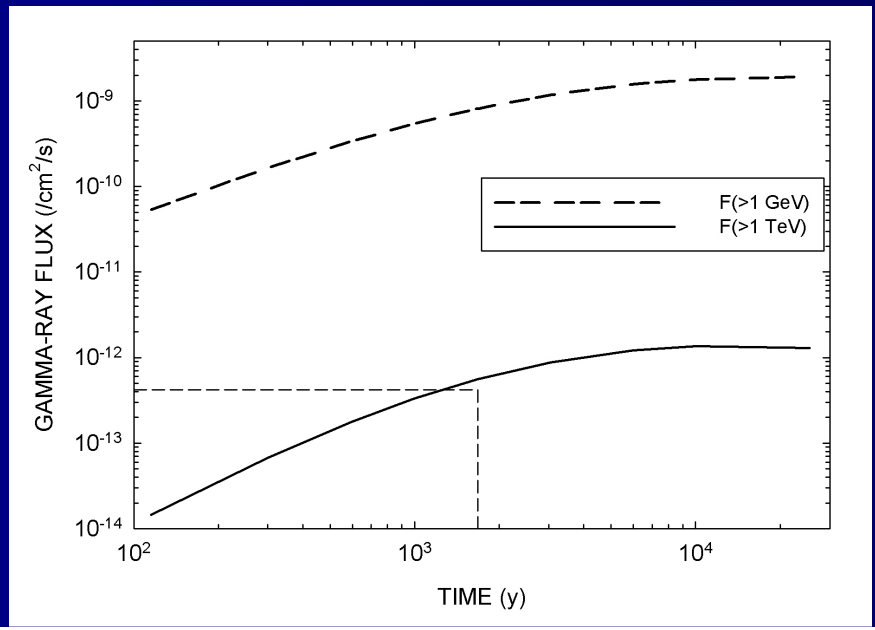

The Possenti et al. (2002)
L_X-Edot relationship – X-ray Evolution

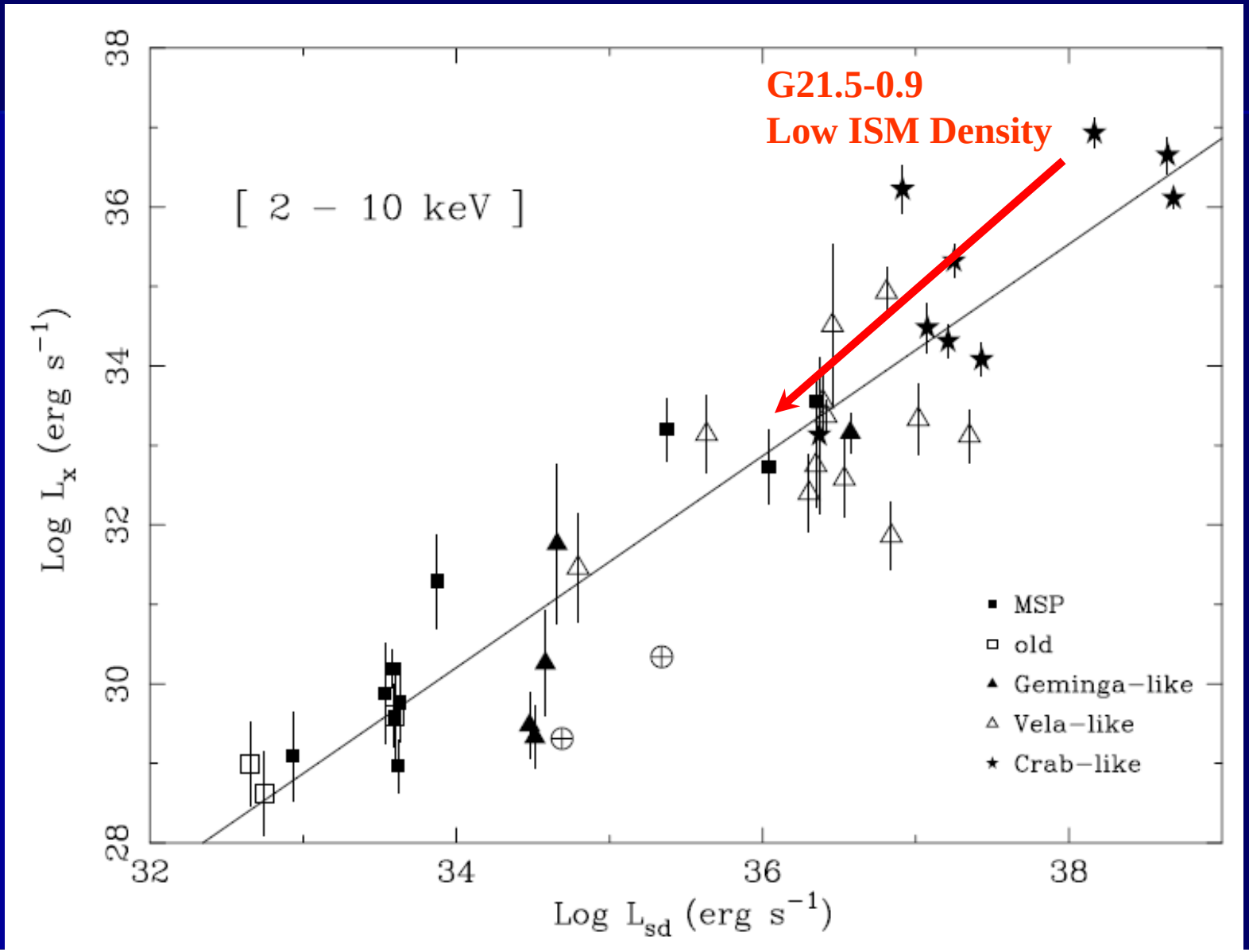

Hessels et al. (2008) TeV/Edot Conversion Efficiency – TeV Evolutionary Track

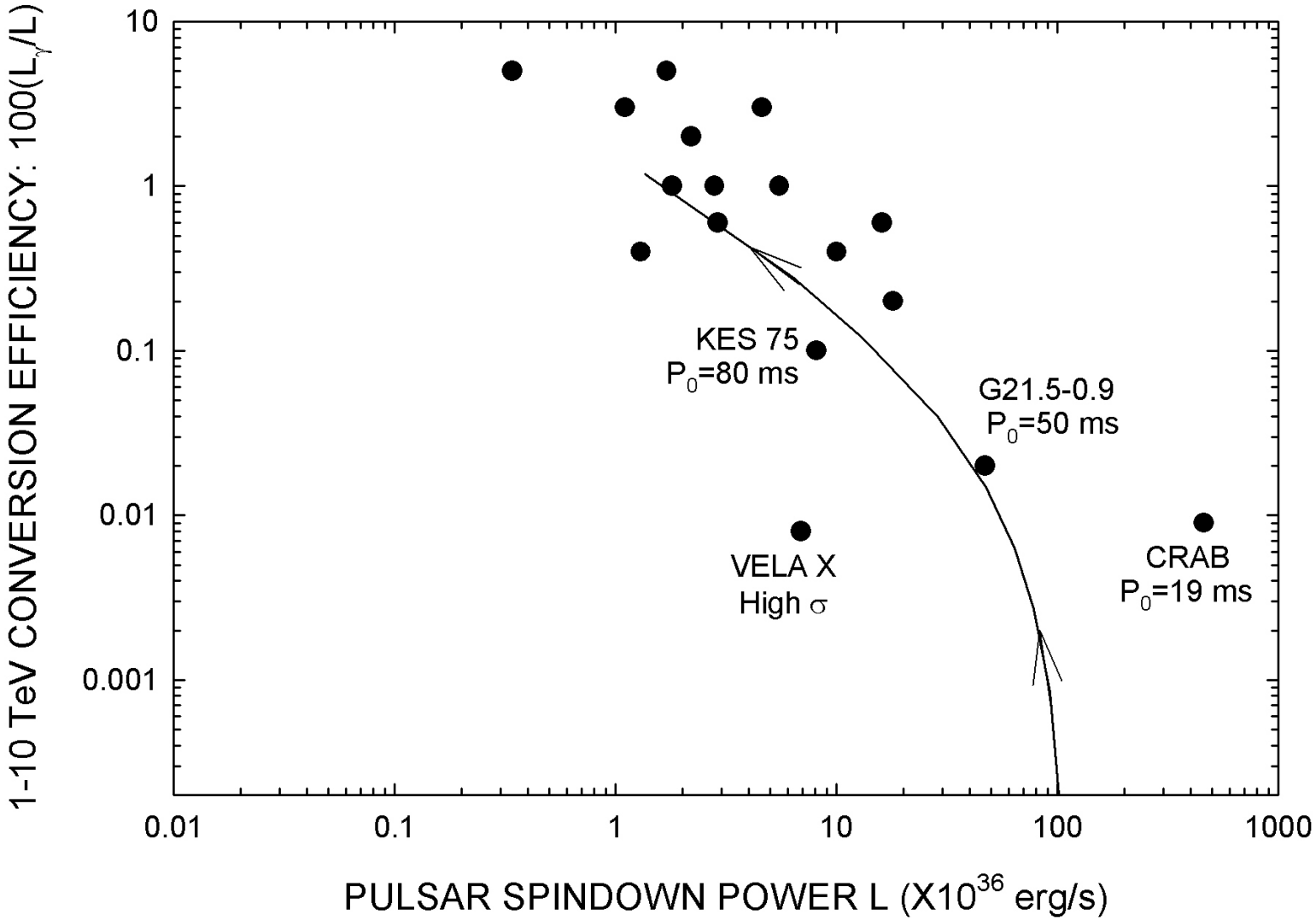

The Calirometric-Relic Effect

When the lifetime of radiating particles

$$\tau(E_\gamma) \sim (4.8\ \mathrm{kyr}) \left(\frac{B_\perp}{10^{-5}\ \mathrm{G}}\right)^{-2} E_{\mathrm{TeV}}^{-1/2}.$$

$$\tau(E_\gamma) \sim \frac{(100\ \mathrm{kyr})}{[1 + 0.144(B_{\mu\mathrm{G}})^2] E_{\mathrm{TeV}}^{1/2}},$$

exceeds the pulsar spindown timescale by a large amount

$$\tau = \frac{3Ic^3}{\Omega_i^2 B_{ns}^2 R_{ns}^6 \sin^2\alpha},$$

The apparent conversion efficiency may exceed 100%

If the neutron star surface field strength times the birth rotational frequency is large enough, the pulsar spins down rapidly and may leave an **Unidentified Gamma-Ray Source** with uninteresting pulsar counterpart!

KES 75 (Djannati-Atai et al. 2007)

- $R_{PWN}=0.6d_6$ pc; $R_{SNR}=2.8d_6$ pc
- Requires $n\approx20$ cm^{-3} (Leahy & Tan 2007)
- R_{PWN}/R_{SNR} => $P_0=80$ -100 ms (van der Swaluw & Wu 2001)
- $T_{age}\approx800$ yr.
- $\int(-\dot{E})dt \approx 2 \times10^{48}$ erg for $L_0=8\times10^{38}$ erg/s.
- H.E.S.S. observations give field strength below equipartition $B\approx15$ μG or $W_B=2\times10^{44}$ erg (Djannati-Atai et al. 2007; Ng et al. 2008).

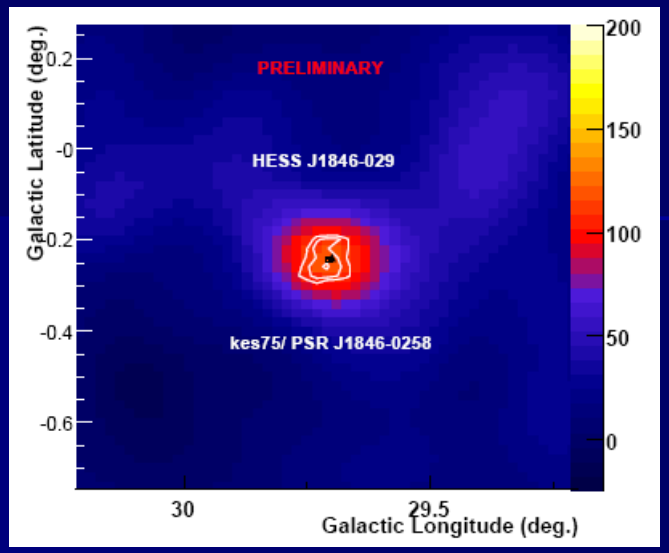

H.E.S.S.: Djannati-Ataï et al. (2007)

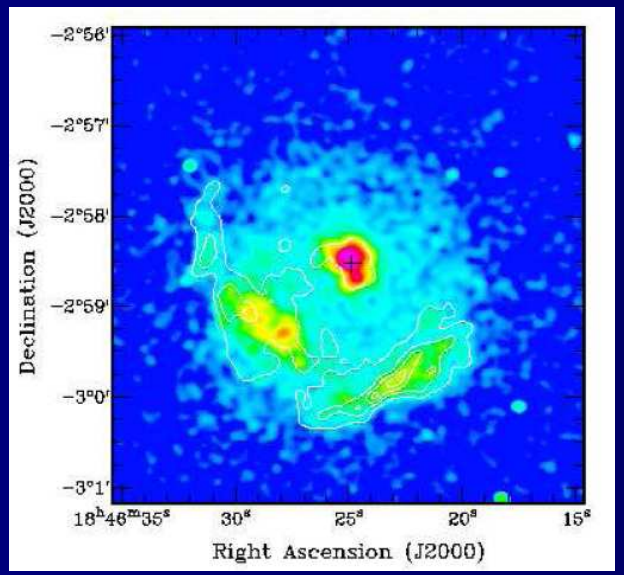

CHANDRA: Helfand et al. (2002)

Time dependent injection model for MWL spectrum of KES 75 – Observed radio flux consistent with P_0 = 80 ms and H.E.S.S. determined field strength. Intrinsic break energy 40 GeV – consistent with X-ray and VHE gamma-ray observations.

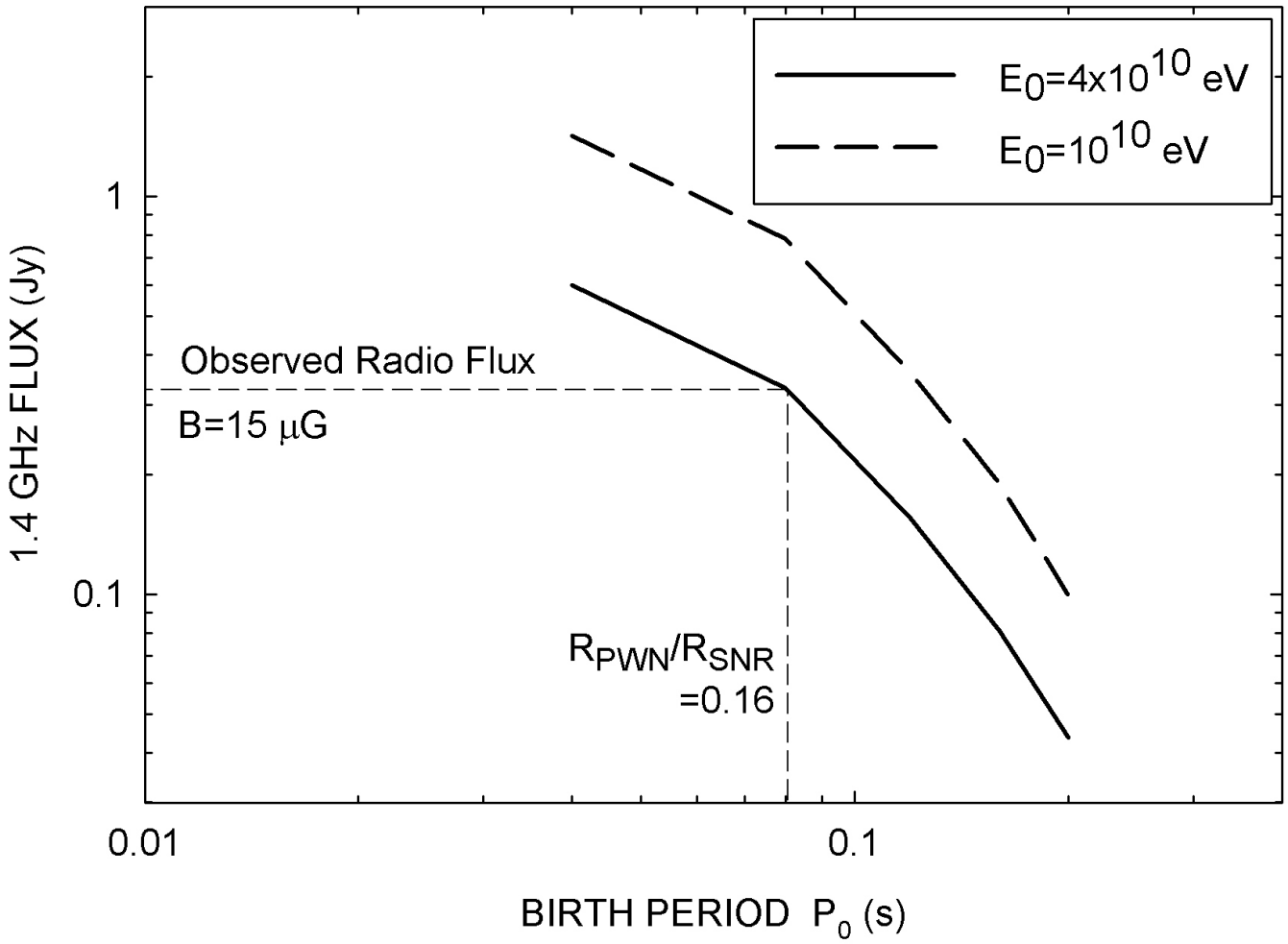

Time dependent model for MWL spectrum of KES 75. Radiation break energy smeared by variable field strength.

35% Conversion efficiency of spindown power to leptons

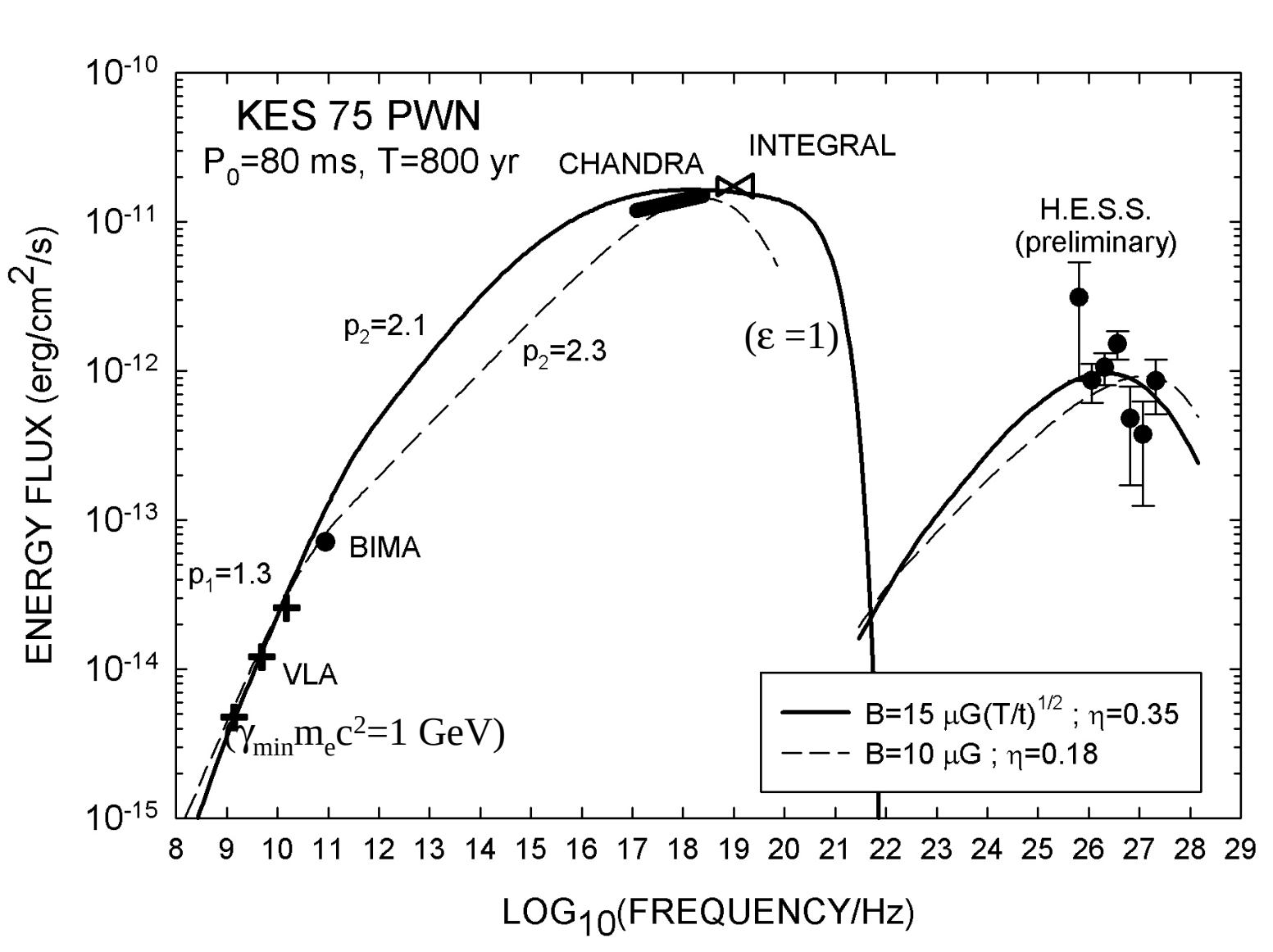

KES 75 Results

- Energy in field: $W_B=2\times10^{44}$ erg (same as Ng et al. 2008)
- Total particle energy of $W_E=3.4\times10^{47}$ erg $\approx 0.17 \int(-\dot{E})dt$ (some fraction lost to radiation). Clearly particle dominated, unlike Crab Nebula! Small avg. sigma.
- Total number of leptons: $N_e>8\times10^{48}$ (1 GHz radio frequency lower limit from 1 GeV $e^{\pm}$)
- Integrated number of Goldreich Julian pairs: $N_{GJ}=1.6\times10^{44}$
- Pair production multiplicity (upper limit from electron energy lower limit of 1 MeV): $2.5\times10^5 > M > 2.4\times10^4$

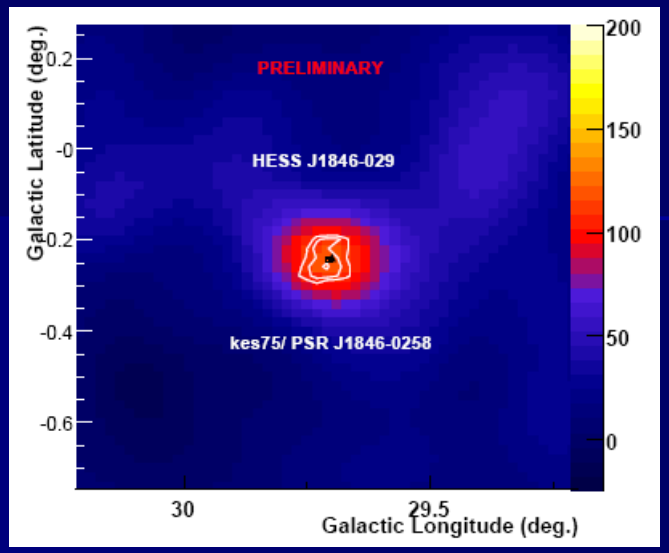

H.E.S.S.: Djannati-Ataï et al. (2007)

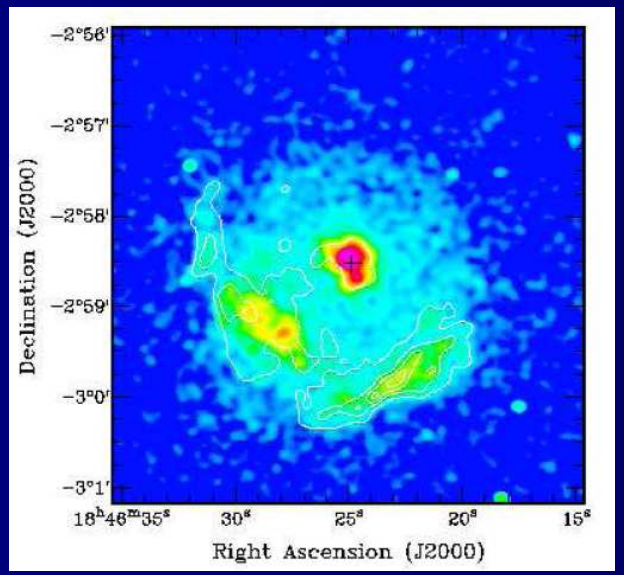

CHANDRA: Helfand et al. (2002)

Conclusions

- GeV-TeV emission gives us a handle on macroscopic evolutionary quantities.
- Wide FoV X-ray surveys important.
- Pair production multiplicities are $2.5 \times 10^5 > M > 2.4 \times 10^4$ for KES 75 and $2.2 \times 10^5 > M > 0.9 \times 10^5$ for G21.5-0.9 are exceptional.
- Density of ISM has an impact on the evolution of X-ray to VHE gamma-ray luminosity.
- Some unidentified TeV sources may be old PWN with
  - Relatively high B_{NS}/P_0 (calirometric relic effect) and
  - Low ISM density